

Ubiquitous Asymptotic Robustness in Biochemical Systems

Hyukpyo Hong^{*1}, Diego Rojas La Luz^{†1}, and Gheorghe Craciun^{‡1,2}

¹Department of Mathematics, University of Wisconsin–Madison

²Department of Biomolecular Chemistry, University of Wisconsin–Madison

Abstract

Living systems maintain stable internal states despite environmental fluctuations. Absolute concentration robustness (ACR) is a striking homeostatic phenomenon in which the steady-state concentration of a molecular species remains entirely invariant to changes in total molecular supply. Although experimental studies have reported approximate—but not exact—robustness in steady-state concentrations, such behavior has often been attributed to exact ACR motifs perturbed by measurement noise or minor side reactions, rather than recognized as a structural property of the network itself. In this work, we highlight a previously underappreciated phenomenon, which we term *asymptotic ACR* (or *aACR*): approximate robustness can emerge solely from the architecture of the reaction network, without requiring parameters being negligible or the presence of an exact ACR motif. We find that aACR is far more common than classical ACR, as demonstrated in systems such as the *Escherichia coli* EnvZ-OmpR system and MAPK signaling cascade. Furthermore, we mathematically prove that such ubiquity stems solely from network structures. Finally, we reveal a counterintuitive feature of aACR in systems with multiple conserved quantities, revealing subtle distinctions in how robustness manifests in complex biochemical networks.

Introduction

Biological systems possess a remarkable ability to maintain precise concentrations of key molecules despite environmental fluctuations, and it is essential for sustaining life [1–7]. This robustness is observed across diverse biochemical contexts, including the Calvin cycle [8], the EnvZ-OmpR osmoregulation system, various metabolic pathways in *Escherichia coli* (*E. coli*) [9–11], and pyrimidine metabolism in plants [12–14]. Understanding the principles that underlie this robustness remains a central objective in systems biology. Many studies have uncovered structural mechanisms that confer such robustness [15–18], including control-theoretic approaches for robust perfect adaptation [4, 19–21] and structural sensitivity analyses that are independent of reaction kinetics [22–27].

A notable milestone in this line of work is the concept of absolute concentration robustness (ACR), introduced by Shinar and Feinberg [28, 29]. Specifically, a species is said to have ACR if the steady-state concentration of the species remains exactly invariant to changes in initial conditions. The

^{*}hhong78@wisc.edu

[†]rojaslaluz@wisc.edu

[‡]craciun@wisc.edu

authors also provided structural sufficient condition for a network having a species with ACR, based on chemical reaction network theory. This sparked a series of investigations on necessary conditions for ACR [30, 31], its dynamical stability [32, 33], stochastic formulations [34, 35], and broader theoretical frameworks [36, 37].

Previous studies primarily analyze robustness of the steady-state concentration of a certain species X , here denoted by X^{ss} , with respect to perturbations in another quantity Y (e.g., rate constant, initial condition, or conserved quantity), seeking conditions under which X^{ss} remains strictly constant. These efforts have established mathematical foundations for understanding mechanisms where X^{ss} remains *completely* constant despite changes in Y . However, an equally biologically relevant phenomenon—*approximate* concentration robustness, where X^{ss} remains *nearly* invariant—has been unacknowledged. Although such approximate robustness has been frequently observed in experiments [9, 10], it is often dismissed as an artifact of experimental noise or attributed to negligible-rate reactions within a surrounding “core” ACR network, rather than being recognized as a structural property in its own right. This has led prior studies to focus narrowly on strict, complete robustness.

In this work, we introduce the concept of *asymptotic* ACR (aACR), showing that approximate robustness can arise purely from the architecture of a reaction network, independent of kinetic parameters and even without a core ACR module. We first demonstrate that aACR more accurately reflects experimental observations than conventional ACR, and illustrate the underlying mechanism using a simple, representative network. Our results reveal that aACR is ubiquitous and thus substantially more common than conventional ACR, as evidenced by detailed analysis of the *E. coli* EnvZ-OmpR and IDHKP-IDH glyoxylate bypass regulation system, phospho-dephosphorylation futile cycle, and the Goldbeter–Koshland module for MAPK signaling cascade. We further prove a mathematical theorem that implies this ubiquitous phenomenon arises generically from structural features of biochemical networks, without requiring parameter fine-tuning. Along with the theorem, we provide a method that allows identifying every steady-state behavior whether it has aACR or not. Finally, we emphasize the importance of rigorous aACR analysis in the presence of multi-dimensional environmental perturbations, as the system’s response can exhibit counterintuitive behavior under such conditions.

Results

Realistic experimental outputs require consideration of approximate concentration robustness.

A common experimental approach to studying concentration robustness involves measuring how the steady-state concentration of an output species Y responds as the initial concentration of an input species X is systematically varied. This procedure yields a dose-response curve, offering insights into the robustness of the system. Specifically, the initial concentration of X is systematically varied (e.g., 1 mM, 2 mM, 3mM, ...) (Figure 1a), and the respective steady-state concentration of Y is measured using a detection device (Figure 1b). The resulting data points are plotted to create a dose-response curve, which reveals how Y responds to changes in X . If the measured concentrations of Y are nearly identical across all test tubes, despite the varying initial concentrations of X , one can conclude that Y exhibits concentration robustness, as its concentration remains stable under perturbations to X (Figure 1c). This experimental setup motivates two key considerations for defining and analyzing concentration robustness. First, in real-world experiments, it is often impractical to vary all initial conditions simultaneously. Instead, experimental protocols typically involve changing one input species at a time while holding others constant [38]. This practical constraint suggests that robustness should be defined

with respect to specific input species or conserved quantities, rather than requiring invariance across all possible initial conditions. Second, experimental noise and the limited resolution of measurements make it difficult to distinguish between perfect robustness (where the output concentration is exactly the same) and approximate robustness (where the output concentration is nearly but not exactly the same). In both cases, the dose-response curve (i.e., input-output curve) may appear identical, as shown in Figure 1c.

These observations highlight the need for a more nuanced definition of concentration robustness that captures both perfect and near-perfect behaviors. While traditional definitions of ACR require the output concentration to be exactly the same across all initial conditions, this condition is often too stringent to apply in experimental settings. Instead, we propose a new framework that focuses on *asymptotic* ACR (aACR), where the output concentration approaches a fixed value as the input concentration is increased. This definition not only aligns more with realistic experimental settings but also allows us to identify and analyze systems that exhibit approximate concentration robustness, which may be more prevalent in real-world biological networks. By grounding our analysis in this experimental perspective, we aim to bridge the gap between theoretical models and practical measurements, providing a more realistic framework for studying robustness in biological systems.

ACR and aACR are practically indistinguishable.

To illustrate the classical concept of ACR and our newly proposed concept of aACR and their differences, we analyze a very simple reaction network with two species X and Y and two reactions (Figure 2a). The first reaction, $X + Y \rightarrow 2Y$, is an autoactivation reaction where an inactive form of an enzyme, X , is activated by interacting with an active form, Y . The second reaction, $Y \rightarrow X$, is inactivation of the active form Y . Since there is no pure production or decay of the enzymes, the total concentration of enzymes is always a constant, i.e., $X(t) + Y(t) = X(0) + Y(0) = T$ for all $t \geq 0$ where $X(t)$ and $Y(t)$ represent the concentrations of the species X and Y at time t , respectively, with a slight abuse of notation. Dynamics of the concentrations $X(t)$ and $Y(t)$ can be described by the following differential equations:

$$\begin{aligned}\frac{dX(t)}{dt} &= -\alpha X(t)Y(t) + \beta Y(t), \\ \frac{dY(t)}{dt} &= \alpha X(t)Y(t) - \beta Y(t),\end{aligned}\tag{1}$$

where α and β are the rate constants for the activation and inactivation reactions, respectively (Figure 2a).

The time evolution of the concentrations can be depicted on the phase plane (Figure 2b). On the phase plane of this reaction network, every point with positive initial concentrations of both X and Y eventually converge to the set of steady states (orange lines; Figure 2b). Specifically, except for the small region of low total concentrations (gray region; Figure 2b), every initial point converges to steady states lying on a vertical line (red dotted line; Figure 2b). That is, wherever an initial point is, its steady state has the same concentration of X . This implies that the steady-state concentration of X , denoted by X^{ss} , is independent of the overall supply of this system (i.e., the total enzyme concentration). When this independence appears, we say “ X has ACR.” This phenomenon of ACR is achieved in networks with specific structural properties revealed by Shinar and Feinberg [28]. Consequently, the dose-response curve of X^{ss} with respect to the total enzyme concentration, T , reaches a fixed value (i.e., the horizontal line) once T exceeds a threshold (Figure 2c), which indicates that X admits ACR.

While exhibiting ACR in a certain species serves as a valuable information indicating that the steady-state concentration of the species is completely independent of an initial condition, this property can easily be lost with slight modifications to the network structure. Here, we modify the network in Figure 2a by adding the reverse of the second reaction (Figure 2d). Consequently, the set of steady states and thus the robustness of X^{ss} are altered. Specifically, the set of steady states is not a vertical line but an asymptote (orange curve; Figure 2e) to a vertical line (blue dotted line; Figure 2e). This indicates that the steady-state concentration of X is not exactly a constant, but it approaches a constant asymptotically as the total enzyme concentration increases. Although the steady-state concentration of X is not completely independent of the total concentration T , *its dependence on T is negligible when T is large enough*. (Note that even if X has ACR, X^{ss} *does* depend on T when T is small; see Figure 2c.) Therefore, we say “ X has *aACR* with respect to T ” when this asymptotic independence appears (see Supplementary Information for a precise definition). The dose-response curve of X^{ss} with respect to T reaches a fixed value (i.e., the horizontal line) asymptotically as T becomes large (Figure 2f). Although the two networks do not show the exactly same dose-response curves (Figure 2c,f), it is noteworthy that there is no meaningful difference for the practical purpose of real experiments. In particular, as illustrated in Figure 1, a dose-response curve is commonly measured with noise and limited data resolution. Thus, it is nearly impossible to distinguish if an observed flat dose-response curve with discrete data points was measured from a perfectly horizontal line with ACR (Figure 2c) or a nearly horizontal plateau with aACR (Figure 2f). This highlights that identifying networks showing aACR is as important as identifying networks with ACR. Moreover, this aACR of X appears solely from the network structure (Figure 2d), independently of the rate constant γ of the added reverse reaction.

aACR is (empirically and mathematically) ubiquitous in real biochemical systems.

In the example shown in Figure 2, both ACR and aACR are analyzed in terms of changes to the total concentration T , which is the only conserved quantity in the system. However, there is a subtle but important distinction between the two concepts when considering systems with multiple conserved quantities. The conventional notion of ACR is defined as the property where a species maintains the same steady-state concentration across *all* initial conditions, regardless of how the conserved quantities are varied. In contrast, aACR must be analyzed by varying each conserved quantity individually, as the steady-state behavior of a system may differ depending on which quantity is changed. This distinction did not arise in Figure 2, where there was only one conserved quantity, but it becomes critical in systems like the EnvZ-OmpR network (Figure 3), which has two conserved quantities corresponding to the total concentrations of X -containing and Y -containing species.

To better align with experimental practices, we define aACR *with respect to a specific species*. That is, the steady-state concentration of an output species is analyzed as the initial concentration of a particular input species is varied, while keeping all other initial concentrations fixed. This setup reflects standard experimental protocols for measuring dose-response curves [38], as illustrated in Figure 1. In such experiments, the initial level of one species is systematically varied to observe its effect on a designated target species at steady state. Defining aACR in this manner not only enhances its experimental relevance but also provides a consistent framework for analyzing systems with multiple conserved quantities (see Supplementary Information for detailed definitions).

The EnvZ-OmpR osmoregulation system in *Escherichia coli* is a well-studied example of a two-component signaling network (Figure 3a), where robustness in molecular concentrations plays a critical role in cellular function. This system consists of the sensor kinase EnvZ (denoted as X) and the response regulator OmpR (denoted as Y). Both proteins can exist in phosphorylated forms, X_P and

Y_P , which are central to the signaling process. The kinase X autophosphorylates using adenosine triphosphate (ATP) as a phosphate donor, and X_P subsequently transfers the phosphoryl group to Y , forming Y_P . Dephosphorylation of Y_P is catalyzed by X in the presence of ATP or adenosine diphosphate (ADP). The phosphorylated response regulator Y_P acts as a transcription factor, regulating the expression of genes involved in osmolarity adaptation, making its concentration crucial for proper cellular function.

Importantly, the network conserves the total concentrations of X -containing species, $T_X = X(t) + XT(t) + X_P(t) + X_PY(t) + XTY_P(t)$, and that of Y -containing species, $T_Y = Y(t) + Y_P(t) + X_PY(t) + XTY_P(t)$. Previous studies have shown that this network exhibits ACR in Y_P , meaning that the steady-state concentration of Y_P is independent of initial conditions $X(0)$ and $Y(0)$ and, equivalently, of the total concentrations T_X and T_Y . Consequently, the dose-response curves of the steady-state concentration of Y_P , denoted by Y_P^{SS} , with respect to varying initial conditions $X(0)$ and $Y(0)$ reach a perfect horizontal line (Figure 3b). However, our analysis reveals that other species in the network, such as X_PY , exhibit aACR, indicated by the dose-response curves approaching, but not precisely reaching, a fixed value as $X(0)$ or $Y(0)$ is increasing (Figure 3c). This reveals that aACR is already present in this network, even though it had not been previously recognized. These results underscore the importance of considering aACR when studying biological robustness, as it may be more prevalent than ACR in real-world systems.

Since the condition of a reaction network to achieve ACR revealed in [28] is sensitive to the network structure, we investigate how sensitive ACR is when the network structure is slightly modified. To do this, we made a minimal modification to the EnvZ-OmpR network by adding a reverse reaction to one of its previously irreversible reactions, $XT \rightarrow X_P$ (Figure 3d). This modification is biologically justifiable, as thermodynamic principles suggest that all reactions are reversible, at least over sufficiently long timescales. In the modified network, the behavior of Y_P changes dramatically (Figure 3e). While it previously exhibited ACR, it now either approaches zero when varying $X(0)$ or shows aACR when varying $Y(0)$ (orange and blue curves in Figure 3e). This demonstrates how ACR can be fragile and sensitive to even small network modifications. In contrast, the concentration of X_PY retains its aACR behavior in the modified network (Figure 3f), indicating the prevalence and persistence of this property.

To further investigate these observations, we analyzed the behavior of all species in the network with respect to varying the initial concentration of each species. Tables 1 and 2 summarize these results for the unmodified and modified networks, respectively. The possible behaviors are: ACR, aACR, divergence (denoted by $\nearrow \infty$), or extinction (i.e., approaching 0, denoted by $\searrow 0$). In the unmodified network, ACR is observed only in Y_P as expected, while aACR is prevalent in several other species, including X_PY (Table 1). In the modified network, all instances of ACR disappeared, with some transitioning to aACR and others to even extinction (Table 2). Notably, most instances of aACR persist, verifying its prevalence and relative robustness compared to ACR. These characteristics of aACR can repeatedly be observed in many other modified networks and even other biological systems, including *E. coli* IDHKP-IDH glyoxylate bypass regulation system, the phospho-dephosphorylation futile cycle, and the Goldbeter-Koshland module for MAPK signaling cascade (Figure S1, Tables S1–S18) [28, 39–41]. Furthermore, we mathematically proved that the widespread emergence of aACR arises from intrinsic features of biochemical network structures, independent of parameter fine-tuning. In particular, any system with at least one positive conserved quantity is guaranteed to exhibit aACR. Finally, we revealed a method that can be used to identify all entries in Table 1, without relying on numerical simulations (see Supplementary Information for details).

When multiple conserved quantities exist, aACR should be carefully analyzed.

While aACR provides a more stable and flexible framework for analyzing concentration robustness, it introduces subtleties that do not arise in the case of ACR. Specifically, a species Z may exhibit aACR with respect to a certain species X and another species Y but not with respect to both of them simultaneously. This counterintuitive phenomenon indeed arises in the EnvZ-OmpR network we analyzed. For example, $X_P Y$ exhibits aACR with respect to X and Y but not both of them simultaneously. The dose-response curves for each of the three cases demonstrate this subtlety (Figure 4a). When $X(0)$ is increasing while $Y(0)$ is fixed, the concentration of $X_P Y$ approaches a fixed value (orange curve), demonstrating aACR with respect to X . Similarly, when $Y(0)$ is increasing while $X(0)$ is fixed, $X_P Y$ also exhibits aACR with respect to Y (green curve). However, when both $X(0)$ and $Y(0)$ are increasing simultaneously, the steady-state concentration of $X_P Y$ keeps growing, indicating that $X_P Y$ no longer exhibits aACR. This also explains why the first four cells show aACR but the last two cells show divergence in the $X_P Y^{\text{SS}}$ column in Table 1.

This counterintuitive behavior can be effectively understood using the 3D visualization in Figure 4b. This 3D plot shows the steady-state concentration of $X_P Y$ as a function of $X(0)$ and $Y(0)$. The surface resembles part of a pyramid: if we move parallel to the X -axis or Y -axis, the concentration of $X_P Y$ asymptotically approaches a constant, reflecting aACR with respect to X and Y individually. However, if we move diagonally (i.e., increasing both $X(0)$ and $Y(0)$ simultaneously), the steady-state concentration of $X_P Y$ keeps increasing linearly, illustrating the divergent behavior observed in Figure 4a.

This subtlety is closely tied to the relationship between initial conditions and conserved quantities. In the EnvZ-OmpR network, the total concentrations of X -containing species (T_X) and Y -containing species (T_Y) are conserved. Changing the initial concentration of a species that belongs to only one conservation law (e.g., X or Y) affects only the corresponding conserved quantity. However, changing the initial concentration of a species that belongs to both conservation laws (e.g., XTY_P) affects both T_X and T_Y , leading to the divergent behavior observed in Figure 4. This explains why $X_P Y$ shows aACR in the first five rows but divergent behavior in the last two rows in Table 1.

These observations underscore the importance of carefully defining aACR with respect to specific species or conserved quantities. While aACR provides a more experimentally relevant framework for studying concentration robustness, it requires a nuanced understanding of how initial conditions and conserved quantities interact in a given network. By exploring these subtleties, we are able to gain deeper insights into the behavior of biological systems and the mechanisms underlying concentration robustness.

Discussion

In this work, we introduced the previously unacknowledged notion of aACR. We showed that approximate concentration robustness is not merely the outcome of “exact” ACR obscured by experimental noise or hidden reactions with negligibly small rate constants. Rather, we demonstrated that such approximate robustness, with respect to the overall supply to the system’s components, can emerge directly from network structure itself. Specifically, whenever a network exhibits aACR for a given species, this approximate invariance arises structurally, without requiring the strong assumption of rate constants being negligible (Figure 2). We further showed that aACR is strikingly widespread across biologically relevant systems, including the *E. coli* IDHKP-IDH glyoxylate bypass regulation system and the phosphorylation-dephosphorylation futile cycle, and the MAPK signaling cascade

(Figures 3 and S1 and Tables S1–S18). To establish that this prevalence is not coincidental, we mathematically proved a general theorem showing that aACR arises as a necessary consequence of structural features in networks with conserved quantities. In other words, the ubiquity of aACR is not accidental—it is an inherent, predictable property of network architecture. Lastly, we highlighted a subtle but important aspect of aACR: the presence of aACR with respect to multiple species *individually* does not necessarily imply the same robustness holds *simultaneously* for those species (Figure 4). Although we presented this as a distinguishing feature of aACR, similar behavior may also arise in networks with conventional ACR. Thus, in both ACR and aACR, individual and joint robustness must be carefully distinguished when evaluating system behavior.

While ACR has traditionally been the focus of efforts to identify robustness in reaction networks, our findings suggest that this emphasis may be too narrow. If one seeks only networks exhibiting exact ACR, many biologically relevant systems that display robust behavior in practice will be overlooked. Networks with aACR can maintain stable concentrations of key species over a wide range of conditions, yet they may not satisfy the strict algebraic or structural conditions required for ACR. This underscores the need to broaden our search criteria: by accounting for approximate behaviors that arise intrinsically from network architecture—rather than dismissing them as deviations or noise—we may uncover a wider and more realistic array of candidate networks for engineering or understanding robust biological functions.

Moreover, our results challenge the prejudice that approximate concentration robustness necessarily arises from a “core” ACR subnetwork embedded within a larger system. We have shown that aACR, which is an instance of approximate robustness, can exist even when no identifiable ACR core is present. For example, in Tables 1 and 2, aACR phenomena are frequently observed from the species that are irrelevant to core ACR structure. Furthermore, we examine the phosphorylation-dephosphorylation futile cycle (Figure S1c) and the Goldbeter–Koshland module for MAPK signaling cascade (Figure S1d), and not a single ACR phenomenon is observed while many aACR are found (Tables S13–S18). That is, the behavior cannot be attributed to a subsystem with exact ACR that is merely perturbed by additional reactions or noise. Instead, the robustness emerges from the interplay of reactions across the full network, often involving mechanisms that fall outside the scope of traditional ACR theory. This observation suggests that aACR represents a genuinely distinct form of robustness, so this deserves separate theoretical treatment and recognition in both modeling and experimental analysis.

We studied the deterministic regime (i.e., ODEs) in this work. However, when system components are present in low copy numbers and the randomness of reactions cannot be neglected, the stochastic regime (e.g., continuous-time Markov chains or SDEs) should be considered. In this context, aACR becomes even more important, as a stochastic model must always produce data with approximate concentration robustness by its random nature, regardless of whether the system exhibits ACR or aACR. Investigating aACR in stochastic models would be an interesting avenue for future work, complementing previous studies on stochastic models exhibiting ACR [34, 35].

The concept of aACR also opens up promising avenues for synthetic biology, particularly in the design of biochemical circuits for computing and control. In recent work by Khammash and colleagues [4, 42, 43], as well as by Anderson and Joshi [44], chemical reaction networks have been explored as foundational elements for molecular controllers and logic gates. For such systems to function reliably, intermediate modules must maintain consistent outputs even when connected to downstream components or embedded in larger networks. Our results suggest that aACR is especially well-suited for these modular settings: the output species in an aACR module remains stable despite significant changes to conserved quantities. This insensitivity to upstream or downstream perturbations enables robust signal transmission across modular layers, making aACR an attractive structural design prin-

principle for biochemical computing. As such, aACR could provide the robustness backbone needed to build scalable and fault-tolerant synthetic networks.

Methods

Closed-form steady-state solutions for the examples in Figure 2

We calculate steady-state solutions for the examples in Figure 2. For all detailed derivations and steady-state solutions for the other examples, see Supplementary Information.

1. The archetypal network in Figure 2a. The dynamical system associated to it is the one shown in Eq. (1) as follows.

$$\begin{aligned}\frac{dX(t)}{dt} &= -\alpha X(t)Y(t) + \beta Y(t), \\ \frac{dY(t)}{dt} &= \alpha X(t)Y(t) - \beta Y(t).\end{aligned}\tag{2}$$

Since $dX(t)/dt + dY(t)/dt = 0$, we have the conservation law $T = X(t) + Y(t)$. The positive steady states of this system are given by:

$$(X^{\text{ss}}, Y^{\text{ss}}) = \begin{cases} \left(\frac{\beta}{\alpha}, T - \frac{\beta}{\alpha}\right), & \text{for } T \geq \frac{\beta}{\alpha}, \\ (T, 0), & \text{for } T < \frac{\beta}{\alpha}. \end{cases}\tag{3}$$

2. The modified network in Figure 2d. Now, let us focus on the modified reaction network shown in Figure 2d. The corresponding dynamical system can be described by:

$$\begin{aligned}\frac{dX(t)}{dt} &= -\alpha X(t)Y(t) + \beta Y(t) - \gamma X(t), \\ \frac{dY(t)}{dt} &= \alpha X(t)Y(t) - \beta Y(t) + \gamma X(t).\end{aligned}\tag{4}$$

It is still true that we have $T = X(t) + Y(t)$ constant. The steady state of X in terms of T then is given by:

$$X^{\text{ss}} = \frac{1}{2\alpha}(\beta + \gamma + \alpha T - \sqrt{(\alpha T - \beta + \gamma)^2 + 4\beta\gamma})\tag{5}$$

which as T goes to infinity has a limit of $\frac{\beta}{\alpha}$, which shows that the species X exhibits aACR.

Mathematical criteria for aACR

In addition to numerical simulations, we provide theorems (Theorems 3.1 and 3.3 in Supplementary Information) that give mathematical guarantees for the ubiquity of aACR. These mathematical guarantees are useful because they work for any values of the parameters (such as reaction rate constants) present in the system; also, they do not rely on finding explicit formulas for dose-response functions, which is impractical for large networks.

In Theorem 3.1 we have shown that if a reaction system has a positive conservation law that involves species $X_{j_1}, X_{j_2}, \dots, X_{j_k}$ but *not* species X_i , then *at least one of the species X_j must be aACR with respect to X_i* . In Theorem 3.3 we have shown that if, moreover, certain polynomials (which are obtained via algebraic elimination, and can be computed using standard tools of computational algebraic geometry) do not vanish at the origin, then *all the species $X_{j_1}, X_{j_2}, \dots, X_{j_k}$ must be aACR with respect to X_i* . These results are described in detail in Supplementary Information, together with representative examples that illustrate their application to several biochemically relevant systems. Indeed, this technique allowed us to recalculate all the entries in Table 1 mathematically (as opposed to numerically) and independently validate the results of our numerical simulations.

Author Contributions

Conceptualization: H.H., D.RLL., and G.C. Investigation: H.H., D.RLL., and G.C. Supervision: G.C. Simulation: H.H. Data Analysis: H.H., D.RLL., and G.C. Writing: H.H., D.RLL., and G.C.

Acknowledgments

We thank Balázs Boros for valuable comments and discussions.

This work was made possible in part by the support of the Fulbright Program, which sponsored Diego Rojas La Luz’s doctoral studies in the United States.

Funding: This work was supported in part by the National Science Foundation under grant DMS-2051568.

Competing Interests

The authors declare no competing interests.

Figures and Tables

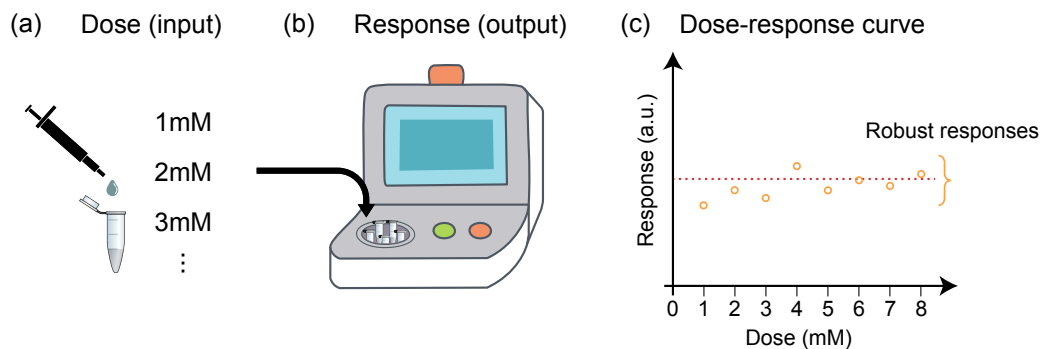


Figure 1: Illustration of an experimental setup for assessing concentration robustness. (a) A series of experiments is conducted by varying the concentration of the dose (i.e., input species). (b) The corresponding steady-state concentrations of the response (i.e., the output species) are measured. (c) The input–output pairs are used to construct a dose–response curve. If the output concentrations remain similar despite changes in the input, the system is considered to exhibit concentration robustness of the output species with respect to the input species.

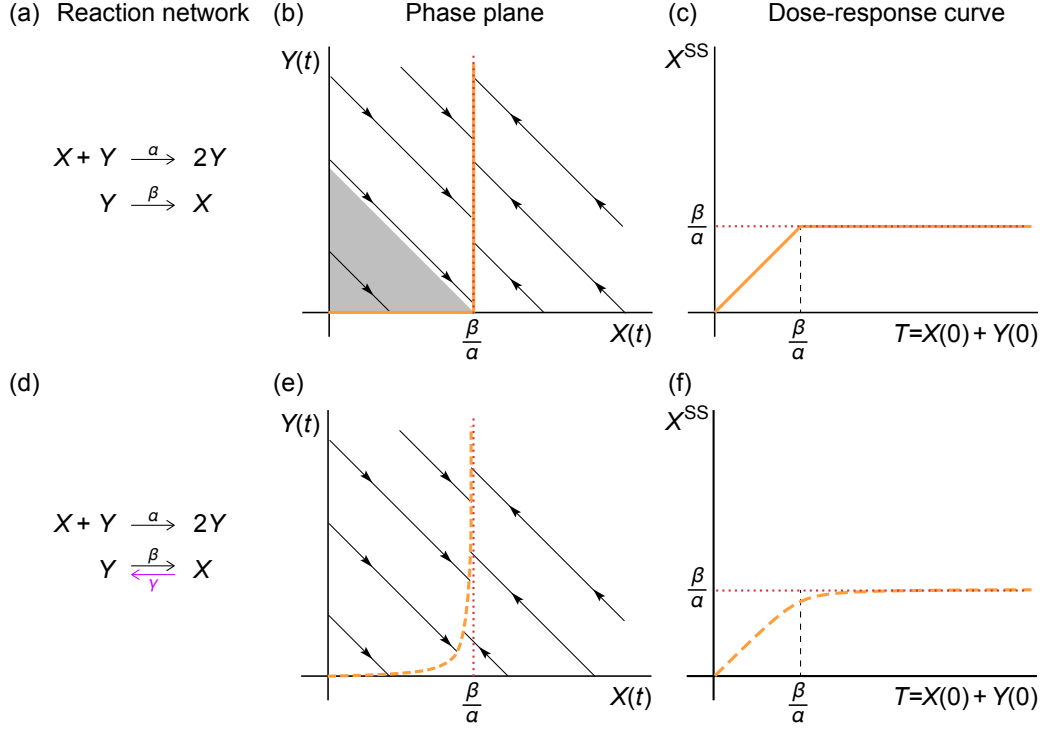


Figure 2: Simple reaction networks possessing ACR vs. asymptotic ACR (aACR). (a) A reaction network with two reactions $X + Y \rightarrow 2Y$ and $Y \rightarrow X$. (b) The phase plane describing the dynamics of this reaction network. Orange lines represent the set of steady states. Except for the initial values on the small gray region, all steady-state concentrations of X are exactly the same value (red dotted line). Here, $X(t)$ and $Y(t)$ denote the concentrations of X and Y at time t . (c) The dose-response curve of the steady-state concentration of X , denoted by X^{ss} , with respect to the conserved quantity in the reaction network, $T = X(0) + Y(0)$. Except for the initial increment, X^{ss} remains constant. (d) A reaction network modified from (a) by adding one more reaction, $X \rightarrow Y$. (e) The phase-plane of the modified network in (d). The perfect vertical shape of the set of steady-state in (b) disappeared, but still the steady-state concentrations of X form a curve that converges asymptotically to the vertical red dotted line. Here, the orange line being dashed represents its asymptotic behavior. (f) The same dose-response curve as in (c) with the modified reaction network. Although X^{ss} no longer becomes a constant function, it converges to the same value. Notably, the two dose-response curves in (c) and (f) are nearly indistinguishable.

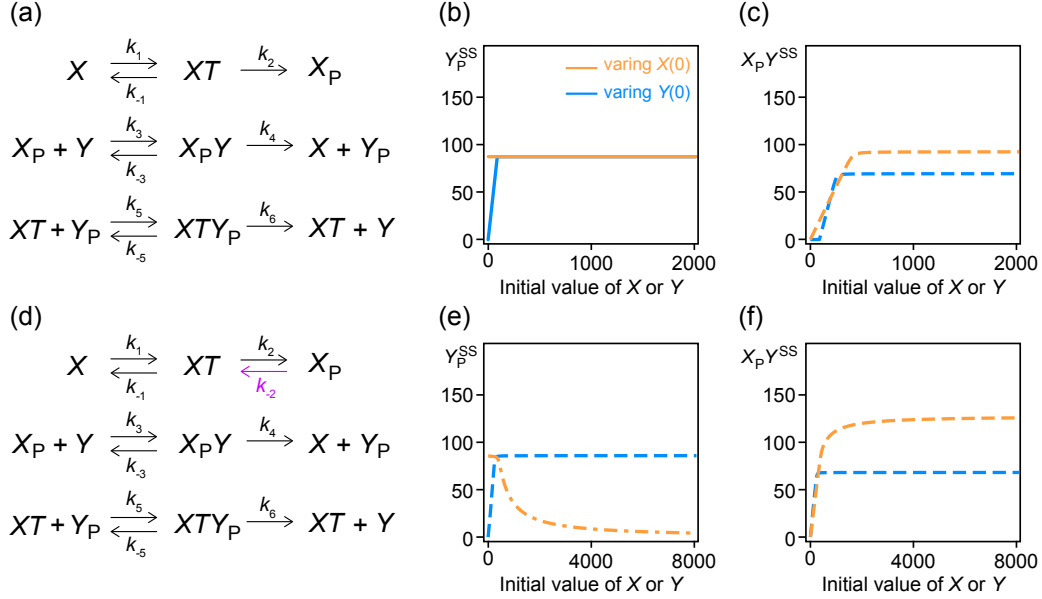


Figure 3: Biologically relevant networks showing ACR and aACR phenomena. (a) The EnvZ-OmpR signaling network, a well-studied biochemical system, serves as a key example of a network with ACR in species Y_P . (b) Dose-response curves for Y_P show that its steady-state concentration reaches a fixed value (horizontal line) when varying the initial concentration of X (orange curve) or Y (blue curve), demonstrating ACR. Here, Y_P^{SS} , $X(0)$, and $Y(0)$ denote the steady-state concentration of Y_P and the initial values of X and Y , respectively. Note that these two curves overlap as they reach the same Y_P^{SS} value. (c) In contrast, $X_P Y$ exhibits aACR, denoted by dashed lines. This is demonstrated by the dose-response curve of its steady-state concentration, denoted by $X_P Y^{SS}$, approaching but never precisely reaching a fixed value as the initial concentrations of X or Y are increasing. (d) A network modified from the network in (a) by making one irreversible reaction, $XT \rightarrow X_P$, reversible. (e) In this modified network, Y_P no longer exhibits ACR: its steady-state concentration, Y_P^{SS} , approaches zero when varying $X(0)$ and shows aACR when varying $Y(0)$. (f) Despite this modification, $X_P Y$ retains aACR, highlighting the robustness of this property compared to ACR.

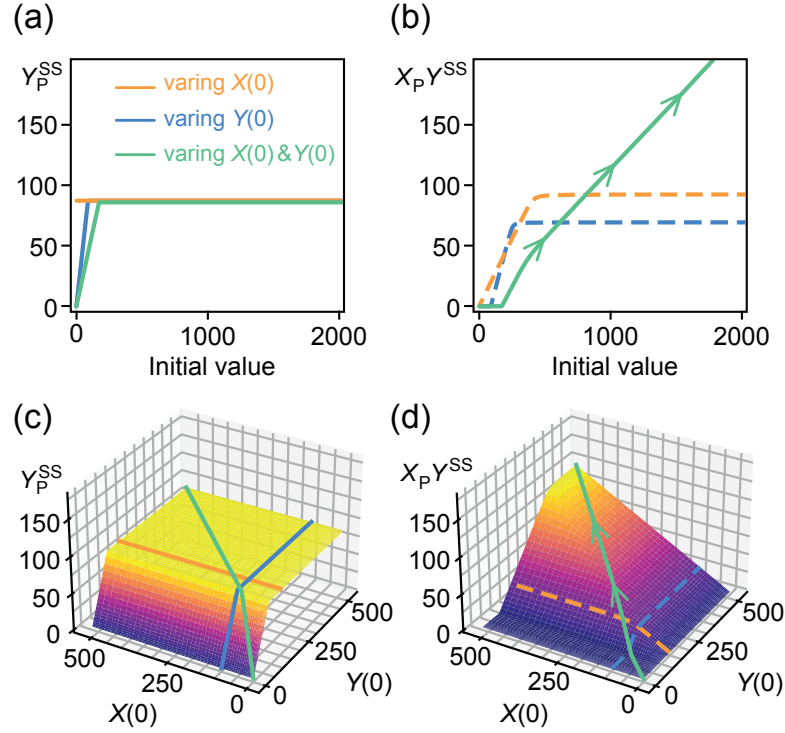


Figure 4: A subtlety of aACR, observed in Figure 3c. (a) One additional dose-response curve is added to Figure 3b, demonstrating ACR of Y_P . When both of $X(0)$ and $Y(0)$ are varying, Y_P still exhibits ACR. (b) One additional dose-response curve is added to Figure 3c. Although $X_P Y_P^{SS}$ shows aACR with respect to each of $X(0)$ and $Y(0)$, unexpectedly, $X_P Y_P^{SS}$ keeps increasing when both of $X(0)$ and $Y(0)$ are simultaneously varying. (c) A dose-response “surface” of Y_P^{SS} . The three colored lines are corresponding to those in (a). They reach the completely flat plateau, indicating ACR of Y_P . (d) A dose-response surface of $X_P Y_P^{SS}$. Unlike the surface in (c), this surface does not have a plateau; instead, it looks like a pyramid. While the two dashed lines asymptotically reach a finite constant along the lateral faces, the green curve keeps increasing along the (diagonal) lateral edge.

	X^{ss}	XT^{ss}	X_P^{ss}	Y^{ss}	Y_P^{ss}	$X_P Y^{ss}$	XY_P^{ss}
$X(0)$	aACR	aACR	$\nearrow \infty$	$\searrow 0$	ACR	aACR	aACR
$XT(0)$	aACR	aACR	$\nearrow \infty$	$\searrow 0$	ACR	aACR	aACR
$X_P(0)$	aACR	aACR	$\nearrow \infty$	$\searrow 0$	ACR	aACR	aACR
$Y(0)$	aACR	aACR	$\searrow 0$	$\nearrow \infty$	ACR	aACR	aACR
$Y_P(0)$	aACR	aACR	$\searrow 0$	$\nearrow \infty$	ACR	aACR	aACR
$X_P Y(0)$	$\nearrow \infty$	$\nearrow \infty$	aACR	$\nearrow \infty$	ACR	$\nearrow \infty$	$\nearrow \infty$
$XY_P(0)$	$\nearrow \infty$	$\nearrow \infty$	aACR	$\nearrow \infty$	ACR	$\nearrow \infty$	$\nearrow \infty$

Table 1: Summary of steady-state concentration responses of single species with respect to a increasing initial value of another species for the network in Figure 3a. The four possible behaviors, ACR, aACR, divergence, or extinction (i.e., approaching 0), are denoted by ACR, aACR, $\nearrow \infty$, and $\searrow 0$ in the table. Although the table was obtained from numerical simulation results, all entries can also be identified using a method based on computational algebraic geometry. See Supplementary Information for a detailed description about the method.

	X^{ss}	XT^{ss}	X_P^{ss}	Y^{ss}	Y_P^{ss}	$X_P Y^{ss}$	XY_P^{ss}
$X(0)$	$\nearrow \infty$	$\nearrow \infty$	$\nearrow \infty$	$\searrow 0$	$\searrow 0$	aACR	aACR
$XT(0)$	$\nearrow \infty$	$\nearrow \infty$	$\nearrow \infty$	$\searrow 0$	$\searrow 0$	aACR	aACR
$X_P(0)$	$\nearrow \infty$	$\nearrow \infty$	$\nearrow \infty$	$\searrow 0$	$\searrow 0$	aACR	aACR
$Y(0)$	aACR	aACR	$\searrow 0$	$\nearrow \infty$	aACR	aACR	aACR
$Y_P(0)$	aACR	aACR	$\searrow 0$	$\nearrow \infty$	aACR	aACR	aACR
$X_P Y(0)$	$\nearrow \infty$	$\nearrow \infty$	aACR	$\nearrow \infty$	aACR	$\nearrow \infty$	$\nearrow \infty$
$XY_P(0)$	$\nearrow \infty$	$\nearrow \infty$	aACR	$\nearrow \infty$	aACR	$\nearrow \infty$	$\nearrow \infty$

Table 2: Summary of steady-state concentration responses for the network in Figure 3d. The yellow-colored cells show where the steady-state behavior has changed when compared with the unmodified network, while transparent cells have the same steady-state behaviors as the unmodified network (see Table 1.) A majority of the steady-state behaviors are maintained after this modification.

References

- [1] H. Kitano, “Biological robustness,” *Nature Reviews Genetics*, vol. 5, no. 11, pp. 826–837, 2004.
- [2] H. Kitano, “Towards a theory of biological robustness,” *Molecular systems biology*, vol. 3, no. 1, p. 137, 2007.
- [3] U. Alon, M. G. Surette, N. Barkai, and S. Leibler, “Robustness in bacterial chemotaxis,” *Nature*, vol. 397, no. 6715, pp. 168–171, 1999.
- [4] S. K. Aoki, G. Lillacci, A. Gupta, A. Baumschlager, D. Schweingruber, and M. Khammash, “A universal biomolecular integral feedback controller for robust perfect adaptation,” *Nature*, vol. 570, no. 7762, pp. 533–537, 2019.
- [5] N. Barkai and S. Leibler, “Robustness in simple biochemical networks,” *Nature*, vol. 387, no. 6636, pp. 913–917, 1997.
- [6] D. S. Goldstein, “How does homeostasis happen? integrative physiological, systems biological, and evolutionary perspectives,” *American Journal of Physiology-Regulatory, Integrative and Comparative Physiology*, vol. 316, no. 4, pp. R301–R317, 2019. PMID: 30649893.
- [7] U. Alon, *An introduction to systems biology: design principles of biological circuits*. Chapman and Hall/CRC, 2019.
- [8] D. F. Wilson and F. M. Matschinsky, “Metabolic homeostasis in life as we know it: Its origin and thermodynamic basis,” *Frontiers in Physiology*, vol. Volume 12 - 2021, 2021.
- [9] E. Batchelor and M. Goulian, “Robustness and the cycle of phosphorylation and dephosphorylation in a two-component regulatory system,” *Proceedings of the National Academy of Sciences*, vol. 100, no. 2, pp. 691–696, 2003.
- [10] D. C. LaPorte, P. E. Thorsness, and D. E. Koshland, “Compensatory phosphorylation of isocitrate dehydrogenase. a mechanism for adaptation to the intracellular environment.,” *Journal of Biological Chemistry*, vol. 260, no. 19, pp. 10563–10568, 1985.
- [11] N. Ishii, K. Nakahigashi, T. Baba, M. Robert, T. Soga, A. Kanai, T. Hirasawa, M. Naba, K. Hirai, A. Hoque, *et al.*, “Multiple high-throughput analyses monitor the response of e. coli to perturbations,” *Science*, vol. 316, no. 5824, pp. 593–597, 2007.
- [12] L. Bellin, F. Del Caño-Ochoa, A. Velázquez-Campoy, T. Möhlmann, and S. Ramón-Maiques, “Mechanisms of feedback inhibition and sequential firing of active sites in plant aspartate transcarbamoylase,” *Nature Communications*, vol. 12, no. 947, pp. 1–13, 2021.
- [13] J. v. R. Henry Christopher and V. d. E. Wim, “Functional analysis of the pyrimidine de novo synthesis pathway in solanaceous species,” *Plant Physiology*, vol. 138, no. 4, pp. 1926–1938, 2005.
- [14] P. Geigenberger, B. Regierer, A. Nunes-Nesi, A. Leisse, E. Urbanczyk-Wochniak, F. Springer, J. T van Dongen, J. Kossmann, and A. Fernie, “Inhibition of de novo pyrimidine synthesis in growing potato tubers leads to a compensatory stimulation of the pyrimidine salvage pathway and a subsequent increase in biosynthetic performance,” *Plant Cell*, vol. 17, no. 7, pp. 2077–2088, 2005.

- [15] Y. Hart and U. Alon, “The utility of paradoxical components in biological circuits,” *Molecular Cell*, vol. 49, no. 2, pp. 213–221, 2013.
- [16] Y. Wang, Z. Huang, F. Antoneli, and M. Golubitsky, “The structure of infinitesimal homeostasis in input–output networks,” *Journal of mathematical biology*, vol. 82, no. 7, pp. 1–43, 2021.
- [17] G. Shinar, R. Milo, M. R. Martínez, and U. Alon, “Input–output robustness in simple bacterial signaling systems,” *Proceedings of the National Academy of Sciences*, vol. 104, no. 50, pp. 19931–19935, 2007.
- [18] G. Shinar, U. Alon, and M. Feinberg, “Sensitivity and robustness in chemical reaction networks,” *SIAM Journal on Applied Mathematics*, vol. 69, no. 4, pp. 977–998, 2009.
- [19] M. H. Khammash, “Perfect adaptation in biology,” *Cell Systems*, vol. 12, no. 6, pp. 509–521, 2021.
- [20] A. Gupta and M. Khammash, “Universal structural requirements for maximal robust perfect adaptation in biomolecular networks,” *Proceedings of the National Academy of Sciences*, vol. 119, no. 43, p. e2207802119, 2022.
- [21] R. P. Araujo and L. A. Liotta, “The topological requirements for robust perfect adaptation in networks of any size,” *Nature communications*, vol. 9, no. 1, pp. 1–12, 2018.
- [22] T. Okada and A. Mochizuki, “Sensitivity and network topology in chemical reaction systems,” *Phys. Rev. E*, vol. 96, p. 022322, Aug 2017.
- [23] T. Okada and A. Mochizuki, “Law of localization in chemical reaction networks,” *Phys. Rev. Lett.*, vol. 117, p. 048101, Jul 2016.
- [24] H. Hong, S. Moon, Y. Hirano, and J. K. Kim, “Topological criterion for robust perfect adaptation of reaction fluxes in biological networks,” *iScience*, 2025/04/16 XXXX.
- [25] A. Mochizuki and B. Fiedler, “Sensitivity of chemical reaction networks: A structural approach. 1. examples and the carbon metabolic network,” *Journal of Theoretical Biology*, vol. 367, pp. 189 – 202, 2015.
- [26] B. Fiedler and A. Mochizuki, “Sensitivity of chemical reaction networks: a structural approach. 2. regular monomolecular systems,” *Mathematical Methods in the Applied Sciences*, vol. 38, no. 16, pp. 3519–3537, 2015.
- [27] A. Ferjani, K. Kawade, M. Asaoka, A. Oikawa, T. Okada, A. Mochizuki, M. Maeshima, M. Y. Hirai, K. Saito, and H. Tsukaya, “Pyrophosphate inhibits gluconeogenesis by restricting udp-glucose formation in vivo,” *Scientific Reports*, vol. 8, p. 14696, Oct 2018.
- [28] G. Shinar and M. Feinberg, “Structural sources of robustness in biochemical reaction networks,” *Science*, vol. 327, no. 5971, pp. 1389–1391, 2010.
- [29] J. Gunawardena, “Biological systems theory,” *Science*, vol. 328, no. 5978, pp. 581–582, 2010.
- [30] G. Shinar and M. Feinberg, “Design principles for robust biochemical reaction networks: What works, what cannot work, and what might almost work,” *Mathematical Biosciences*, vol. 231, no. 1, pp. 39–48, 2011. Special issue on biological design principles.

- [31] J. M. Eloundou-Mbebi, A. Küken, N. Omranian, S. Kleessen, J. Neigenfind, G. Basler, and Z. Nikoloski, “A network property necessary for concentration robustness,” *Nature communications*, vol. 7, no. 1, pp. 1–7, 2016.
- [32] B. Joshi and G. Craciun, “Foundations of static and dynamic absolute concentration robustness,” *Journal of Mathematical Biology*, vol. 85, no. 5, p. 53, 2022.
- [33] B. Joshi and G. Craciun, “Reaction network motifs for static and dynamic absolute concentration robustness,” *SIAM Journal on Applied Dynamical Systems*, vol. 22, no. 2, pp. 501–526, 2023.
- [34] D. F. Anderson, D. Cappelletti, and T. G. Kurtz, “Finite time distributions of stochastically modeled chemical systems with absolute concentration robustness,” *SIAM Journal on Applied Dynamical Systems*, vol. 16, no. 3, pp. 1309–1339, 2017.
- [35] D. F. Anderson, G. A. Enciso, and M. D. Johnston, “Stochastic analysis of biochemical reaction networks with absolute concentration robustness,” *Journal of The Royal Society Interface*, vol. 11, no. 93, p. 20130943, 2014.
- [36] R. L. Karp, M. P. Millán, T. Dasgupta, A. Dickenstein, and J. Gunawardena, “Complex-linear invariants of biochemical networks,” *Journal of theoretical biology*, vol. 311, no. 21, pp. 130–138, 2012.
- [37] L. D. García Puente, E. Gross, H. A. Harrington, M. Johnston, N. Meshkat, M. Pérez Millán, and A. Shiu, “Absolute concentration robustness: Algebra and geometry,” *Journal of Symbolic Computation*, vol. 128, p. 102398, 2025.
- [38] J. Haas, J. Manro, H. Shannon, W. Anderson, J. Brozinick, A. Chakravartty, M. Chambers, J. Du, B. Eastwood, J. Heuer, *et al.*, “In vivo assay guidelines,” *Assay Guidance Manual [Internet]*, 2012.
- [39] C. Conradi and C. Pantea, “Multistationarity in biochemical networks: results, analysis, and examples,” in *Algebraic and combinatorial computational biology*, pp. 279–317, Elsevier, 2019.
- [40] A. Goldbeter and D. E. Koshland Jr, “An amplified sensitivity arising from covalent modification in biological systems.,” *Proceedings of the National Academy of Sciences*, vol. 78, no. 11, pp. 6840–6844, 1981.
- [41] B. N. Kholodenko, “Negative feedback and ultrasensitivity can bring about oscillations in the mitogen-activated protein kinase cascades,” *European journal of biochemistry*, vol. 267, no. 6, pp. 1583–1588, 2000.
- [42] G. Lillacci, Y. Benenson, and M. Khammash, “Synthetic control systems for high performance gene expression in mammalian cells,” *Nucleic Acids Research*, vol. 46, pp. 9855–9863, 09 2018.
- [43] S. Anastassov, M. Filo, C.-H. Chang, and M. Khammash, “A cybergenetic framework for engineering intein-mediated integral feedback control systems,” *Nature Communications*, vol. 14, p. 1337, Mar 2023.
- [44] D. F. Anderson and B. Joshi, “Chemical mass-action systems as analog computers: implementing arithmetic computations at specified speed,” *Theoret. Comput. Sci.*, vol. 1025, pp. Paper No. 114983, 23, 2025.

Supplementary Information: Ubiquitous Asymptotic Robustness in Biochemical Systems

Hyukpyo Hong^{*1}, Diego Rojas La Luz^{†1}, and Gheorghe Craciun^{‡1,2}

¹Department of Mathematics, University of Wisconsin–Madison

²Department of Biomolecular Chemistry, University of Wisconsin–Madison

1 Definitions

Notational Remark. Throughout this document, we use both $A(t)$ and $[A](t)$ to denote the concentration of species A at time t . The time argument “ (t) ” is often omitted when no confusion arises. Square brackets are employed to distinguish between expressions like $[A][B]$ and $[AB]$ in the presence of species A , B , and their binding complex AB . For notational convenience, we use both \bar{A} (or $[\bar{A}]$) and A^{ss} to represent the steady-state concentration of species A .

Definition 1.1. Consider a reaction system on the nonnegative orthant $\mathbb{R}_{\geq 0}^n$ and a concentration vector $\mathbf{x}_0 \in \mathbb{R}_{\geq 0}^n$. The compatibility class that contains the initial concentration \mathbf{x}_0 is the set of all state vectors in $\mathbb{R}_{\geq 0}^n$ that satisfy the same linear conservation relations as \mathbf{x}_0 .

Definition 1.2. We say that a reaction system has well defined dose-response curves for input X_i if there exists a unique positive equilibrium within the compatibility class that contains the initial concentration $\mathbf{x}_0 + \lambda \mathbf{e}_i$ for all λ large enough, where \mathbf{e}_i is the i^{th} element of the standard basis of \mathbb{R}^n . The function that maps the number λ to the j^{th} coordinate of the equilibrium vector within compatibility class of $\mathbf{x}_0 + \lambda \mathbf{e}_i$ is called the dose-response curve of X_j with respect to X_i . That is, this function maps λ to $\bar{X}_j(\lambda)$.

Definition 1.3. Consider a reaction system that has well defined dose-response curves for input X_i . A species X_j is said to admit asymptotic ACR (aACR) with respect to X_i and has aACR value $a_{i,j} > 0$ if for any $\mathbf{x}_0 \in \mathbb{R}_{\geq 0}^n$, we have

$$\lim_{\lambda \rightarrow \infty} \bar{X}_j(\lambda) = a_{i,j}, \quad (\text{S1})$$

where $\bar{X}_j(\lambda)$ is the steady state of species X_j for the system with initial concentration $\mathbf{x}_0 + \lambda \mathbf{e}_i$. In words, we say X_i admits aACR if the dose-response curve of X_j with respect to X_i converges to a positive real number as $\lambda \rightarrow \infty$.

2 Model-specific derivation and analysis for the archetypal example in Figure 2a

Consider first the reaction network in Figure 2a. The dynamical system associated to it is the one shown in Equation (1) in the main text. For the sake of simplicity, we will omit the time-dependence when calculating $X(t)$ and $Y(t)$. Thus we have

$$\begin{aligned} \frac{dX}{dt} &= -\alpha XY + \beta Y, \\ \frac{dY}{dt} &= \alpha XY - \beta Y. \end{aligned} \quad (\text{S2})$$

^{*}hhong78@wisc.edu

[†]rojaslaluz@wisc.edu

[‡]craciun@wisc.edu

From these equations, we get the conservation law as

$$\frac{dX}{dt} + \frac{dY}{dt} = 0, \quad (\text{S3})$$

which shows that $T = X(t) + Y(t)$ will be constant. Now, to find the steady state variety, it will be given by taking

$$\frac{dX}{dt} = -\frac{dY}{dt} = 0, \quad (\text{S4})$$

so we have

$$-\alpha X^{\text{ss}} Y^{\text{ss}} + \beta Y^{\text{ss}} = 0, \quad (\text{S5})$$

$$(-\alpha X^{\text{ss}} + \beta) Y^{\text{ss}} = 0, \quad (\text{S6})$$

thus, either $Y^{\text{ss}} = 0$ or $-\alpha X^{\text{ss}} + \beta = 0$. Using that $X^{\text{ss}} + Y^{\text{ss}} = T$ we get

$$X^{\text{ss}} = \frac{\beta}{\alpha}, \quad Y^{\text{ss}} = -\frac{\beta}{\alpha} + T, \quad (\text{S7})$$

$$X^{\text{ss}} = T, \quad Y^{\text{ss}} = 0. \quad (\text{S8})$$

Now, let us focus on the modified reaction network shown in Figure 2d. The corresponding dynamical system can be described by:

$$\begin{aligned} \frac{dX}{dt} &= -\alpha XY + \beta Y - \gamma X, \\ \frac{dY}{dt} &= \alpha XY - \beta Y + \gamma X. \end{aligned} \quad (\text{S9})$$

It is still true that we have $T = X(t) + Y(t)$ constant. The steady state variety now is given by

$$-\alpha X^{\text{ss}} Y^{\text{ss}} + \beta Y^{\text{ss}} - \gamma X^{\text{ss}} = 0. \quad (\text{S10})$$

Using $T = X^{\text{ss}} + Y^{\text{ss}}$, we can substitute and calculate the steady states in terms of T :

$$X^{\text{ss}} = \frac{1}{2\alpha}(\beta + \gamma + \alpha T - \sqrt{\Delta}), \quad (\text{S11})$$

$$Y^{\text{ss}} = \frac{1}{2\alpha}(-\beta - \gamma + \alpha T + \sqrt{\Delta}), \quad (\text{S12})$$

where

$$\Delta = \beta^2 + \gamma^2 + \alpha^2 T^2 + 2\beta\gamma + 2\alpha\gamma T - 2\alpha\beta T, \quad (\text{S13})$$

$$= (\alpha T - \beta + \gamma)^2 + 4\beta\gamma. \quad (\text{S14})$$

Note that this solution is unique with the restriction that both $A, B \geq 0$. We then see that as $T \rightarrow \infty$, $\sqrt{\Delta} \rightarrow \alpha T - \beta + \gamma$ and so

$$X^{\text{ss}} \approx \frac{1}{2\alpha}(\beta + \gamma + \alpha T - (\alpha T - \beta + \gamma)) = \frac{\beta}{\alpha}. \quad (\text{S15})$$

Note that here we calculated X^{ss} in terms of T , but if X_i is either X or Y , then as λ goes to infinity, T also goes to infinity. Thus the limit of $X^{\text{ss}}(\lambda)$ is positive and finite, which analytically shows the species X exhibits aACR with respect to either X or Y .

Remark 2.1. *Note that we have an even stronger result in this case. Specifically, if we compute the steady-state variety over all of \mathbb{R}^2 and separate the stable and unstable varieties, then as $\gamma \rightarrow 0$, the stable variety of (S9) approaches uniformly to the stable variety of in Equation (1) in the main text. The same holds for the respective unstable varieties.*

3 Theorems that ensure ubiquity of aACR in biochemical systems

Consider a reaction system given by

$$\begin{aligned}\frac{dX_1}{dt} &= f_1(X_1, \dots, X_n) \\ &\vdots \\ \frac{dX_n}{dt} &= f_n(X_1, \dots, X_n)\end{aligned}\tag{S16}$$

where $f_i(X_1, \dots, X_n)$ are rational functions, with conservation laws

$$\begin{aligned}\sum_{i=1}^n \alpha_i^{(1)} X_i(t) &= \sum_{i=1}^n \alpha_i^{(1)} X_i(0) \\ &\vdots \\ \sum_{i=1}^n \alpha_i^{(m)} X_i(t) &= \sum_{i=1}^n \alpha_i^{(m)} X_i(0)\end{aligned}\tag{S17}$$

Our main theorem (Theorem 3.1) essentially states that any positive conservation law with proper support can be used to guarantee the following: for any species X_i that *does not* show up in the conservation law, there exists at least one species X_j that *does* show up in it and admits aACR.

Theorem 3.1. *Consider a reaction system given by (S16) that has well defined dose-response curves for input X_i . Assume that this system admits a positive conservation law with support set $\Sigma = \{X_{j_1}, \dots, X_{j_k}\}$, such that X_i is not in Σ . Then there exists at least one species X_j within Σ such that X_j admits aACR with respect to X_i .*

In order to prove this theorem we first discuss a useful lemma.

Lemma 3.2. *Let $P(x, \lambda)$ be a polynomial with real variables x and λ , and consider a continuous function $x(\lambda)$ that satisfies $P(x(\lambda), \lambda) = 0$ for $\lambda > \lambda_0$ big enough. Then $\lim_{\lambda \rightarrow \infty} x(\lambda)$ exists (within the closed interval $[-\infty, \infty]$).*

Moreover, let us write

$$P(x, \lambda) = \lambda^m q(x) + r(x, \lambda),\tag{S18}$$

where m is the highest degree of λ in $P(x, \lambda)$, $q(x)$ is non-zero, and the degree of λ in $r(x, \lambda)$ is less than m . Then, if the limit is finite, it is a root of $q(x)$.

Proof of Lemma 3.2. To show that the limit exists it is enough to prove that

$$\liminf_{\lambda \rightarrow \infty} x(\lambda) = \limsup_{\lambda \rightarrow \infty} x(\lambda).\tag{S19}$$

Write $P(x, \lambda)$ as

$$P(x, \lambda) = \lambda^m q(x) + r(x, \lambda),\tag{S20}$$

where m is the highest degree of λ in $P(x, \lambda)$, $q(x)$ is non-zero, and the degree of λ in $r(x, \lambda)$ is less than m .

Note that if $m = 0$, then $P(x, \lambda) = P(x)$ and so $x(\lambda)$ can only be finitely many values, so it must be constant. Thus in this case the limit exists.

We will assume now that $m > 0$. Then, for $x(\lambda)$,

$$\lambda^m q(x(\lambda)) + r(x(\lambda), \lambda) = 0\tag{S21}$$

$$q(x(\lambda)) + \frac{1}{\lambda^m} r(x(\lambda), \lambda) = 0.\tag{S22}$$

Suppose by contradiction that $\liminf_{\lambda \rightarrow \infty} x(\lambda) = c_1$ is different than $\limsup_{\lambda \rightarrow \infty} x(\lambda) = c_2$, with $c_1, c_2 \in [-\infty, \infty]$. Then, for all $c \in (c_1, c_2)$, there exists a sequence $\lambda_k \rightarrow \infty$ such that

$$\lim_{k \rightarrow \infty} x(\lambda_k) = c \quad (\text{S23})$$

by the Intermediate Value Theorem. Then, in the limit $\frac{1}{\lambda^m} r(x(\lambda), \lambda) = 0$ because $x(\lambda)$ is bounded. But then, as $q(x)$ is a polynomial, it is continuous, so

$$\lim_{k \rightarrow \infty} q(x(\lambda_k)) = q(c) = 0, \quad (\text{S24})$$

which would imply c is a root of q for all $c \in (c_1, c_2)$, a contradiction, as this means $q(x) \equiv 0$, which is not true by construction. Thus, the limit exists, and if it is finite, it must be a root of $q(x)$. \square

We are now ready to proceed to the proof of Theorem 3.1.

Proof of Theorem 3.1. Recall that X_j has aACR with respect to X_i if the steady-state value of X_j , denoted by $\bar{X}_j(\lambda)$, has a finite and positive limit as $\lambda \rightarrow \infty$; see Definition 1.3. Here, λ represents the initial concentration of X_i , which we treat as an “input” value, and the “output” is the corresponding steady-state value of X_j .

For sufficiently large λ , let $\bar{X}(\lambda) = (\bar{X}_1(\lambda), \dots, \bar{X}_n(\lambda))$ denote the unique positive equilibrium in the compatibility class of $\mathbf{x}_0 + \lambda \mathbf{e}_i$. With this notation, $\bar{X}_j(\lambda)$ represents the dose–response curve of X_j with respect to X_i .

We first want to show that the function $\bar{X}_j(\lambda)$ satisfies the properties that are enjoyed by of the function $x(\lambda)$ from the statement of Lemma 3.2, i.e., it is a continuous algebraic function for λ large enough. Note that $\bar{X}(\lambda)$ is a solution of the system of polynomial (steady-state) equations and conservation relations given by

$$\begin{aligned} f_1(\bar{X}(\lambda)) &= 0 \\ &\vdots \\ f_n(\bar{X}(\lambda)) &= 0 \\ \sum_{k=1}^n \alpha_k^{(1)} \bar{X}_k(\lambda) &= C^{(1)} + \alpha_i^{(1)} \lambda \\ &\vdots \\ \sum_{k=1}^n \alpha_k^{(m)} \bar{X}_k(\lambda) &= C^{(m)} + \alpha_i^{(m)} \lambda \end{aligned} \quad (\text{S25})$$

where we can assume f_i are polynomials without loss of generality.

Since the function $\bar{X}(\lambda)$ is a semi-algebraic function (solution of a polynomial system with some sign conditions), and $\bar{X}_j(\lambda)$ is it obtained from it by projection, it follows that $\bar{X}_j(\lambda)$ is a semi-algebraic function by the Tarski–Seidenberg theorem [1]. Then, the graph of $\bar{X}_j(\lambda)$ is a semi-algebraic set, and can be written as a finite union of points and curves that admit parameterizations via diffeomorphisms to the interval $(0, 1)$ (see for example section 3 and especially Corollary 3.8 in [2]). In particular, since the number of such curves is finite, it follows that for λ large enough the graph of $\bar{X}_j(\lambda)$ consists of a single such curve. If we denote this curve by $\gamma(s) = (g(s), h(s))$, then we have

$$\bar{X}_j(g(s)) = h(s),$$

for all $s \in (0, 1)$. But, since $\gamma(s)$ is a diffeomorphism, and the graph of $\bar{X}_j(\lambda)$ satisfies the vertical line test, it follows that $g(s)$ must be one-to-one, and therefore a homeomorphism. Then we obtain

$$\bar{X}_j(\lambda) = h(g^{-1}(\lambda)),$$

and therefore $\overline{X}_j(\lambda)$ is continuous for λ large enough. The fact that $\overline{X}_j(\lambda)$ is an algebraic function (i.e., there exists a nonzero polynomial $P(x, \lambda)$ such that $P(\overline{X}_j(\lambda), \lambda) = 0$) follows similarly from classical properties of semi-algebraic functions. A short but detailed explanation appears for example in the proof of Proposition 2.11 in [2].

We can now conclude that the function $\overline{X}_j(\lambda)$ satisfies the hypotheses of Lemma 3.2, and therefore the limit

$$\lim_{\lambda \rightarrow \infty} \overline{X}_j(\lambda)$$

exists; moreover, since the species X_j is contained in the support of a positive conservation law that does not change as λ changes, it follows that this limit is finite.

If we assume that this limit is zero for all $\overline{X}_j \in \Sigma$, then we arrive at a contradiction: it would imply that each X_j is identically zero for all time, which is impossible due to the conservation laws. Therefore, there must exist at least one species $\overline{X}_j \in \Sigma$ for which the limit $\lim_{\lambda \rightarrow \infty} \overline{X}_j(\lambda)$ is finite and positive. This, in turn, implies that there exists at least one X_j that has aACR with respect to X_i . \square

Remark 3.1. If $P(\overline{X}_j(\lambda), \lambda)$ does not depend on λ , that is, $m = 0$, then X_j admits exact ACR with respect to X_i . In other words, we have not only the following limit:

$$\lim_{\lambda \rightarrow \infty} \overline{X}_j(\lambda) = c \in (0, \infty), \quad (\text{S26})$$

but also that $\overline{X}_j(\lambda) = c$ for all sufficiently large $\lambda > 0$.

Remark 3.2. Recall from the proof of Lemma 3.2 that any finite limit of X_j must be a root of the polynomial $q(x)$ introduced there. From this property we see the following:

If the polynomial $q(x)$ for X_j does not have any non-negative roots, then we must have

$$\lim_{\lambda \rightarrow \infty} \overline{X}_j(\lambda) = \infty. \quad (\text{S27})$$

Similarly, if $q(x)$ for X_j does not have $x = 0$ as a root (which is often the case), then

$$0 < \lim_{\lambda \rightarrow \infty} \overline{X}_j(\lambda) \leq \infty. \quad (\text{S28})$$

Also note that if X_j appears in the support of a positive conservation law, then it is guaranteed to have a finite limit:

$$0 \leq \lim_{\lambda \rightarrow \infty} \overline{X}_j(\lambda) < \infty. \quad (\text{S29})$$

These observations together are particularly useful when establishing that a given species X_j exhibits aACR with respect to X_i , as the following theorem summarizes.

Theorem 3.3. Consider a reaction system given by (S16) that has well defined dose-response curves for input X_i . Assume that this system admits a positive conservation law with support set $\Sigma = \{X_{j_1}, \dots, X_{j_k}\}$, such that X_i is not in Σ . Assume also that X_j is in Σ , and that the polynomial $q(x)$ for X_j does not have a root at zero. Then X_j has aACR with respect to X_i .

Remark 3.3. Note that the polynomial $P(x, \lambda)$ for X_j can be found using Elimination Theory from computational algebraic geometry. In particular, we can use Gröbner basis or resultants to get a explicit polynomial.

3.1 Applications of the theorems to examples

3.1.1 The *Escherichia coli* (*E. coli*) EnvZ-OmpR system.

Example 3.1. Consider the reaction network from Figure 2B in the paper [3] (see Figure 3a in our main text). The corresponding system of ODEs is given by

$$\frac{d[X]}{dt} = -k_1[X] + k_{-1}[XT] + k_3[X_P Y], \quad (\text{S30})$$

$$\frac{d[XT]}{dt} = k_1[X] - (k_{-1} + k_{-1})[XT] - k_{-3}[XT][Y_P] + (k_{-5} + k_4)[XTY_P], \quad (\text{S31})$$

$$\frac{d[X_P]}{dt} = k_{-1}[XT] - k_2[X_P][Y] + k_{-3}[X_P Y], \quad (\text{S32})$$

$$\frac{d[Y]}{dt} = k_4[XTY_P] - k_2[X_P][Y] + k_{-3}[X_P Y], \quad (\text{S33})$$

$$\frac{d[Y_P]}{dt} = k_3[X_P Y] - k_{-3}[XT][Y_P] + k_{-5}[XTY_P], \quad (\text{S34})$$

$$\frac{d[X_P Y]}{dt} = k_2[X_P][Y] - (k_{-3} + k_3)[X_P Y], \quad (\text{S35})$$

$$\frac{d[XTY_P]}{dt} = k_{-3}[XT][Y_P] - (k_{-5} + k_4)[XTY_P]. \quad (\text{S36})$$

This system has two conserved quantities:

- The total mass of *X*-related species: $[X] + [XT] + [X_P] + [X_P Y] + [XTY_P] = T_1$.
- The total mass of *Y*-related species: $[Y] + [Y_P] + [X_P Y] + [XTY_P] = T_2$.

Just from this information, we can apply Theorem 3.1 to conclude the following:

- At least one of the *X*-related species: *X*, *XT*, *X_P*, *X_PY*, or *XTY_P* has aACR with respect to *Y* and similarly for *Y_P*.
- And that one of the *Y*-related species: *Y*, *Y_P*, *X_PY*, or *XTY_P* has aACR with respect to *X* and similarly for *XT* and *X_P*.

Moreover, in this case, we can go further and identify exactly which species exhibit aACR through a more detailed analysis.

First, the steady-state variety formula in terms of $[\overline{X_P Y}]$ and $[\overline{Y}]$ is given by:

$$[\overline{X}] = \frac{(k_{-1} + k_2)k_4[\overline{X_P Y}]}{k_1 k_2} \quad (\text{S37})$$

$$[\overline{XT}] = \frac{k_4[\overline{X_P Y}]}{k_2} \quad (\text{S38})$$

$$[\overline{Y_P}] = \frac{k_2(k_{-5} + k_6)}{k_5 k_6} \quad (\text{S39})$$

$$[\overline{X_P}] = \frac{(k_{-3} + k_4)[\overline{X_P Y}]}{k_3[\overline{Y}]} \quad (\text{S40})$$

$$[\overline{XTY_P}] = \frac{k_4[\overline{X_P Y}]}{k_6}. \quad (\text{S41})$$

Note that $[\overline{Y_P}]$ is independent to $[\overline{XT}]$ and $[\overline{X_P}]$, which indicates the independence to initial conditions. While this formula is the functions of $[\overline{X_P Y}]$ and $[\overline{Y}]$ in addition to rate constants, we can obtain the

formula in terms of T_1 and T_2 , which is more natural. Specifically, from the two conserved quantities,

$$T_1 = [\overline{X}] + [\overline{XT}] + [\overline{X_P}] + [\overline{X_P Y}] + [\overline{XTY_P}] \quad (\text{S42})$$

$$= \frac{(k_{-1} + k_2)k_4[\overline{X_P Y}]}{k_1 k_2} + \frac{k_4[\overline{X_P Y}]}{k_2} + \frac{(k_{-3} + k_4)[\overline{X_P Y}]}{k_3[\overline{Y}]} + [\overline{X_P Y}] + \frac{k_4[\overline{X_P Y}]}{k_6} \quad (\text{S43})$$

$$= \left\{ \frac{(k_{-1} + k_2)k_4}{k_1 k_2} + \frac{k_4}{k_2} + 1 + \frac{k_4}{k_6} \right\} [\overline{X_P Y}] + \frac{(k_{-3} + k_4)}{k_3} \frac{[\overline{X_P Y}]}{[\overline{Y}]}, \quad (\text{S44})$$

$$T_2 = [\overline{Y}] + [\overline{Y_P}] + [\overline{X_P Y}] + [\overline{XTY_P}] \quad (\text{S45})$$

$$= [\overline{Y}] + \frac{k_2(k_{-5} + k_6)}{k_5 k_6} + [\overline{X_P Y}] + \frac{k_4[\overline{X_P Y}]}{k_6} \quad (\text{S46})$$

$$= \frac{k_2(k_{-5} + k_6)}{k_5 k_6} + [\overline{Y}] + \left\{ 1 + \frac{k_4}{k_6} \right\} [\overline{X_P Y}]. \quad (\text{S47})$$

For simplicity of calculations, we rewrite the conservation expressions as

$$T_1 = a[\overline{X_P Y}] + b \frac{[\overline{X_P Y}]}{[\overline{Y}]}, \quad (\text{S48})$$

$$T_2 = c + d[\overline{X_P Y}] + [\overline{Y}], \quad (\text{S49})$$

where a, b, c, d are constants in terms of k_i and in particular c is the ACR value for Y_P .

From this, we can reduce into a single polynomial equation in terms of $[\overline{X_P Y}]$ and T_1, T_2 to then calculate the limit when $X_P Y$ is chosen to be X_j . Indeed, from the second expression,

$$[\overline{Y}] = T_2 - c - d[\overline{X_P Y}], \quad (\text{S50})$$

and after substituting in the first expression and clearing denominators we get

$$a[\overline{X_P Y}](T_2 - c - d[\overline{X_P Y}]) - T_1(T_2 - c - d[\overline{X_P Y}]) + b[\overline{X_P Y}] = 0, \quad (\text{S51})$$

therefore if $X_i \in \{X, XT, X_P\}$, then $T_1 = C_1 + \lambda$, and we get a function $P(x, \lambda)$ for $X_P Y$ evaluated at $x = \overline{X_P Y}(\lambda)$:

$$P([\overline{X_P Y}](\lambda), \lambda) = -\lambda(T_2 - c - d[\overline{X_P Y}](\lambda)) + a[\overline{X_P Y}](\lambda)(T_2 - c - d[\overline{X_P Y}](\lambda)) - T_1(T_2 - c - d[\overline{X_P Y}](\lambda)) + b[\overline{X_P Y}](\lambda) \quad (\text{S52})$$

Thus,

$$q([\overline{X_P Y}](\lambda)) = -(T_2 - c - d[\overline{X_P Y}](\lambda)). \quad (\text{S53})$$

Applying Lemma 3.2 and by Remark 3.2, we see that the limit of $[\overline{X_P Y}](\lambda)$ must be a root of q , so

$$\lim_{\lambda \rightarrow \infty} [\overline{X_P Y}](\lambda) = \frac{T_2 - c}{d}. \quad (\text{S54})$$

Similarly, if $X_i \in \{[\overline{Y}], [\overline{Y_P}]\}$,

$$q([\overline{X_P Y}](\lambda)) = a[\overline{X_P Y}](\lambda) - T_1. \quad (\text{S55})$$

Thus,

$$\lim_{\lambda \rightarrow \infty} [\overline{X_P Y}](\lambda) = \frac{T_1}{a}, \quad (\text{S56})$$

and if $X_i \in \{[X_P Y], [XTY_P]\}$,

$$q([\overline{X_P Y}](\lambda)) = -1. \quad (\text{S57})$$

Therefore, as q does not have any positive roots,

$$\lim_{\lambda \rightarrow \infty} [\overline{X_P Y}](\lambda) = \infty, \quad (\text{S58})$$

by Remark 3.2. Note that using (S50) and (S37) we can deduce the behavior for the other choices of X_j . All of this gives a full description of the Table 1 in our main text.

3.1.2 The phosphorylation-dephosphorylation futile cycle.

Example 3.2. Consider the futile cycle (Figure S1c). It has the following equations:

$$\frac{d[S]}{dt} = -k_1[S][E] + k_{-1}[SE] + k_4[PF], \quad (\text{S59})$$

$$\frac{d[P]}{dt} = -k_3[P][F] + k_{-3}[PF] + k_2[SE], \quad (\text{S60})$$

$$\frac{d[E]}{dt} = -k_1[S][E] + (k_{-1} + k_2)[SE], \quad (\text{S61})$$

$$\frac{d[F]}{dt} = -k_3[P][F] + (k_{-3} + k_4)[PF], \quad (\text{S62})$$

$$\frac{d[SE]}{dt} = k_1[S][E] - (k_{-1} + k_2)[SE], \quad (\text{S63})$$

$$\frac{d[PF]}{dt} = k_3[P][F] - (k_{-3} + k_4)[PF], \quad (\text{S64})$$

with conservation laws

$$[S] + [P] + [SE] + [PF] = T_1, \quad (\text{S65})$$

$$[E] + [SE] = T_2, \quad (\text{S66})$$

$$[F] + [PF] = T_3. \quad (\text{S67})$$

As all the conservation laws are positive, we can use Theorem 3.1 to determine that for each conservation law, there is a species in its support that has aACR with respect to a species not in its support. So for example, using the second conservation law (S66), at least one of E or SE has aACR with respect to S , and similarly for P , F and PF . But, we can do a more detailed analysis by calculating the polynomial equation for a specific species.

Let us analyze the case when $X_j = [SE]$. For this, we will want to reduce the steady-state equations with the conservation laws into a unique polynomial equation only in terms of $[SE]$ and the conservation quantities T_1, T_2, T_3 .

Note that at steady state:

$$[SE] = \frac{k_1}{k_{-1} + k_2} [S][E] = a[S](T_2 - [SE]), \quad (\text{S68})$$

$$[PF] = \frac{k_3}{k_{-3} + k_4} [P][F] = b[P](T_3 - [PF]), \quad (\text{S69})$$

$$[PF] = \frac{k_2}{k_4} [SE] = c[SE], \quad (\text{S70})$$

where $a = \frac{k_1}{k_{-1} + k_2}$, $b = \frac{k_3}{k_{-3} + k_4}$ and $c = \frac{k_2}{k_4}$. Thus, we can express the steady state concentration of all species in terms of $[SE]$:

$$[S] = \frac{[SE]}{a(T_2 - [SE])}, \quad (\text{S71})$$

$$[P] = \frac{c[SE]}{b(T_3 - c[SE])}, \quad (\text{S72})$$

$$[E] = T_2 - [SE], \quad (\text{S73})$$

$$[F] = T_3 - c[SE], \quad (\text{S74})$$

$$[PF] = c[SE]. \quad (\text{S75})$$

Note that for these calculations we used the steady state equations and the second and third conservation laws, but not the first one. Thus, substituting in the first conservation law, we get the reduced polynomial equation:

$$\frac{[SE]}{a(T_2 - [SE])} + \frac{c[SE]}{b(T_3 - c[SE])} + (1 + c)[SE] = T_1 \quad (\text{S76})$$

which reduces to

$$\begin{aligned} & \frac{1}{a}[\overline{SE}]^*(T_3 - c[\overline{SE}]) + \frac{c}{b}[\overline{SE}](T_2 - [\overline{SE}]) \\ & + (1 + c)[\overline{SE}](T_2 - [\overline{SE}])(T_3 - c[\overline{SE}]) - T_1(T_2 - [\overline{SE}])(T_3 - c[\overline{SE}]) = 0. \end{aligned} \quad (\text{S77})$$

Thus, suppose $X_i \in \{S, P\}$, then $T_1 = C_1 + \lambda$, and we obtain a function $P(x, \lambda)$ for SE evaluated at $x = \overline{SE}(\lambda)$:

$$\begin{aligned} P([\overline{SE}](\lambda), \lambda) &= \frac{1}{a}[\overline{SE}](\lambda)(T_3 - c[\overline{SE}](\lambda)) + \frac{c}{b}[\overline{SE}](\lambda)(T_2 - [\overline{SE}](\lambda)) \\ &+ (1 + c)[\overline{SE}](\lambda)(T_2 - [\overline{SE}](\lambda))(T_3 - c[\overline{SE}](\lambda)) - C_1(T_2 - [\overline{SE}](\lambda))(T_3 - c[\overline{SE}](\lambda)) \\ &- \lambda(T_2 - [\overline{SE}](\lambda))(T_3 - c[\overline{SE}](\lambda)). \end{aligned} \quad (\text{S78})$$

From this, we can obtain the function q as follows:

$$q([\overline{SE}](\lambda)) = (T_2 - [\overline{SE}](\lambda))(T_3 - c[\overline{SE}](\lambda)). \quad (\text{S79})$$

Thus, applying Lemma 3.2,

$$\lim_{\lambda \rightarrow \infty} [\overline{SE}](\lambda) = T_2 \text{ or } \frac{T_3}{c}. \quad (\text{S80})$$

From (S71) and (S72), we have natural constraints:

$$[\overline{S}] = \frac{[\overline{SE}]}{a(T_2 - [\overline{SE}])} \geq 0, \quad (\text{S81})$$

$$[\overline{P}] = \frac{c[\overline{SE}]}{b(T_3 - c[\overline{SE}])} \geq 0. \quad (\text{S82})$$

By complying these constraints, the limit of $[\overline{SE}]$ is given as follows:

$$\lim_{\lambda \rightarrow \infty} [\overline{SE}](\lambda) = \min\{T_2, \frac{T_3}{c}\} \in (0, \infty), \quad (\text{S83})$$

and so the species SE exhibits aACR with respect to S or P .

So far, we have analyzed the behavior of the species SE . But, we can use (S71)-(S75) to characterize all possible behaviors of the remaining species using the behavior of SE in the following three distinct cases:

(i) If $T_2 < \frac{T_3}{c}$, then

$$\lim_{\lambda \rightarrow \infty} [\overline{S}](\lambda) = \infty, \quad (\text{S84})$$

$$\lim_{\lambda \rightarrow \infty} [\overline{P}](\lambda) = \frac{cT_2}{b(T_3 - cT_2)} \in (0, \infty), \quad (\text{S85})$$

$$\lim_{\lambda \rightarrow \infty} [\overline{E}](\lambda) = 0, \quad (\text{S86})$$

$$\lim_{\lambda \rightarrow \infty} [\overline{F}](\lambda) = T_3 - cT_2 \in (0, \infty), \quad (\text{S87})$$

$$\lim_{\lambda \rightarrow \infty} [\overline{PF}](\lambda) = cT_2 \in (0, \infty). \quad (\text{S88})$$

In this case, $[P]$, $[F]$, and $[PF]$ admit aACR, while $[S]$ diverges and $[E]$ converges to zero.

(ii) If $T_2 > \frac{T_3}{c}$, then $[S]$, $[E]$, and $[PF]$ admit aACR, while $[P]$ diverges and $[F]$ converges to zero in the limit.

(iii) If $T_2 = \frac{T_3}{c}$, then $[S]$ and $[P]$ both diverge, $[E]$ and $[F]$ converge to zero, and $[PF]$ still admits aACR.

This characterizes the behavior for of each species with respect to $X_i \in \{S, P\}$. By performing a similar analysis for other choices of X_i , we can use the same procedure from (S77) to obtain the full Table S13.

It is noteworthy that even though the behavior is parameter dependent in this example, we can still analyze every possible behavior with our results.

3.1.3 Other networks and network modifications

Even without a detailed analysis, the existence of aACR can often be guaranteed, provided that the conservation laws are known. Moreover, if a network is modified by making an irreversible reaction reversible, such a modification does not alter the conservation laws. As a result, any conclusions drawn from the theorem will continue to hold.

As a first example, note that any modification of the EnvZ-OmpR network (Figure 3a in the main text) will still preserve the same conservation laws.

$$[X] + [XT] + [X_P] + [X_P Y] + [XTY_P] = T_1, \quad (\text{S89})$$

$$[Y] + [Y_P] + [X_P Y] + [XTY_P] = T_2, \quad (\text{S90})$$

and thus, it will still be true by Theorem 3.1 that:

- For each $X_i \in \{Y, Y_P\}$, there is least one $X_j \in \{X, XT, X_P, X_P Y, XTY_P\}$ such that X_j has aACR with respect to X_i .
- For each $X_i \in \{X, XT, X_P\}$, there is least one $X_j \in \{Y, Y_P, X_P Y, XTY_P\}$ such that X_j has aACR with respect to X_i .

This helps explain why aACR will be mostly preserved even if we modify a network by changing irreversible reactions to reversible ones. (See Table 2 in the main text, and Tables S1–S3).

Now, we will analyze the reaction network from Figure 2D in the paper [3] (see Figure S1a). Its conservation laws are

$$[XD] + [X] + [XT] + [X_P] + [X_P Y] + [XDY_P] = T_1, \quad (\text{S91})$$

$$[Y] + [Y_P] + [X_P Y] + [XDY_P] = T_2, \quad (\text{S92})$$

thus, by Theorem 3.1, we see that

- For each $X_i \in \{Y, Y_P\}$, there is least one $X_j \in \{XD, X, XT, X_P, X_P Y, XDY_P\}$ such that X_j has aACR with respect to X_i .
- For each $X_i \in \{XD, X, XT, X_P\}$, there is least one $X_j \in \{Y, Y_P, X_P Y, XDY_P\}$ such that X_j has aACR with respect to X_i .

This is also true for modifications of this network where irreversible reactions are changed to reversible ones (See Tables S4–S8).

Consider now the reaction network from Figure 3 in the paper [3] (see Figure S1b). Its conservation laws are

$$[E] + [EI_P] + [EI_P I] = T_1, \quad (\text{S93})$$

$$[I] + [I_P] + [EI_P] + [EI_P I] = T_2, \quad (\text{S94})$$

thus, by Theorem 3.1, we see that

- For each $X_i \in \{I, I_P\}$, there is least one $X_j \in \{E, EI_P, EI_P I\}$ such that X_j has aACR with respect to X_i .
- For $X_i = E$, there is least one $X_j \in \{Y, Y_P, X_P Y, XDY_P\}$ such that X_j has aACR with respect to X_i .

This is also true for modifications of this network where irreversible reactions are changed to reversible ones (See Tables S9–S12).

Consider the futile cycle reaction network (see Figure S1c). We saw that its conservation laws are

$$[S] + [P] + [SE] + [PF] = T_1, \quad (\text{S95})$$

$$[E] + [SE] = T_2, \quad (\text{S96})$$

$$[F] + [PF] = T_3. \quad (\text{S97})$$

Again, these will not change for its modifications. Note that by Theorem 3.1, we see that

- For each $X_i \in \{E, F\}$, there is least one $X_j \in \{S, P, SE, PF\}$ such that X_j has aACR with respect to X_i .
- For each $X_i \in \{S, P, F, PF\}$, there is least one $X_j \in \{E, SE\}$ such that X_j has aACR with respect to X_i .
- For each $X_i \in \{S, P, E, SE\}$, there is least one $X_j \in \{F, PF\}$ such that X_j has aACR with respect to X_i .

which explains aACR even for the network modifications (See Tables S14–S16).

Finally, consider the Goldbeter-Koshland module for MAPK signaling cascade (see Figure S1d). Its conservation laws are

$$[E_1] + [WE_1] = T_1, \quad (\text{S98})$$

$$[E_2] + [W^*E_2] = T_2, \quad (\text{S99})$$

$$[E_3] + [Z^*E_3] = T_3, \quad (\text{S100})$$

$$[W] + [WE_1] + [W^*] + [W^*E_2] + [ZW^*] = T_4, \quad (\text{S101})$$

$$[Z] + [ZW^*] + [Z^*] + [Z^*E_3] = T_5. \quad (\text{S102})$$

Then, by Theorem 3.1, we see that

- For each $X_i \in \{W, W^*, Z, Z^*, E_2, E_3, W^*E_2, ZW^*, Z^*E_3\}$, there is least one $X_j \in \{E_1, WE_1\}$ such that X_j is aACR with respect to X_i .
- For each $X_i \in \{W, W^*, Z, Z^*, E_1, E_3, WE_1, ZW^*, Z^*E_3\}$, there is least one $X_j \in \{E_2, W^*E_2\}$ such that X_j has aACR with respect to X_i .
- For each $X_i \in \{W, W^*, Z, Z^*, E_1, E_2, WE_1, W^*E_2, ZW^*\}$, there is least one $X_j \in \{E_3, Z^*E_3\}$ such that X_j has aACR with respect to X_i .
- For each $X_i \in \{Z, Z^*, E_1, E_2, E_3, Z^*E_3\}$, there is least one $X_j \in \{W, W^*, WE_1, W^*E_2, ZW^*\}$ such that X_j has aACR with respect to X_i .
- For each $X_i \in \{W, W^*, E_1, E_2, E_3, WE_1, W^*E_2\}$, there is least one $X_j \in \{Z, Z^*, ZW^*, Z^*E_3\}$ such that X_j has aACR with respect to X_i .

See Tables S17 and S18 for the summarized steady-state responses identified from numerical simulations.

4 Supplementary Figures

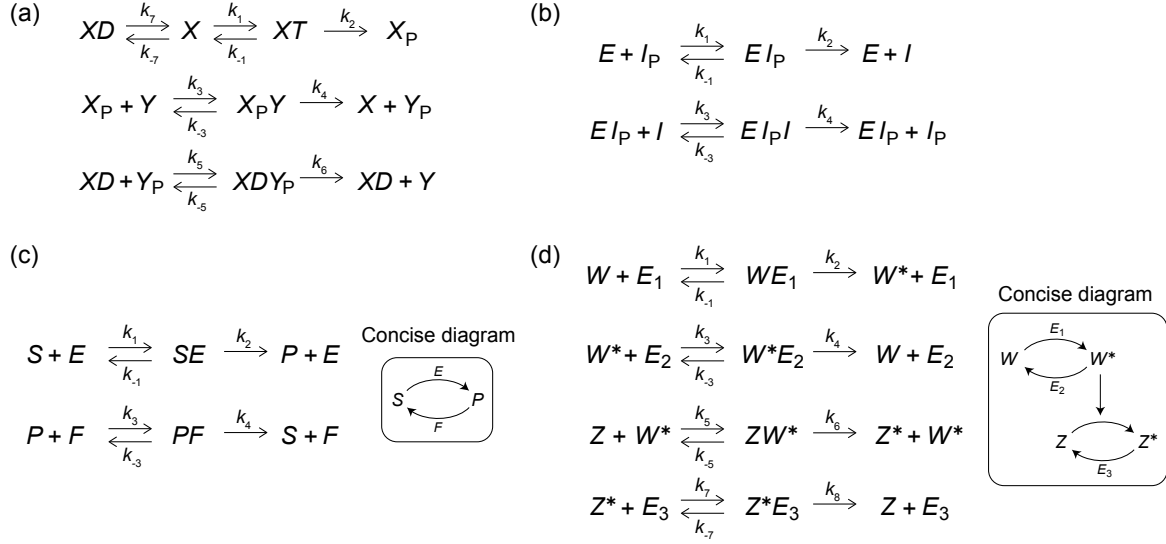


Figure S1: Diagrams of additional examples. (a) A schematic diagram of an *Escherichia coli* (*E. coli*) EnvZ-OmpR model where ADP is the cofactor in phospho-OmpR dephosphorylation. (b) A core absolute concentration robustness (ACR) module in a model of the *E. coli* IDHKP-IDH glyoxylate bypass regulation system. (c) A diagram of a version of the futile cycle, which is a well-studied structure that serves as building blocks in cellular signaling pathways [4]. In the box, we put a concise version that demonstrates why it is called a “futile” cycle. (d) A diagram of the Goldbeter–Koshland module for MAPK signaling cascade [5, 6]. The concise diagram in the box explains why it is called a “cascade.” The diagram structures in (a) and (b) are adopted from Shinar and Feinberg [3].

5 Supplementary Tables

	X^{SS}	XT^{SS}	X_P^{SS}	Y^{SS}	Y_P^{SS}	$X_P Y^{SS}$	XTY_P^{SS}
$X(0)$	aACR	aACR	$\nearrow \infty$	$\searrow 0$	ACR	aACR	aACR
$XT(0)$	aACR	aACR	$\nearrow \infty$	$\searrow 0$	ACR	aACR	aACR
$X_P(0)$	aACR	aACR	$\nearrow \infty$	$\searrow 0$	ACR	aACR	aACR
$Y(0)$	aACR	aACR	$\searrow 0$	$\nearrow \infty$	ACR	aACR	aACR
$Y_P(0)$	aACR	aACR	$\searrow 0$	$\nearrow \infty$	ACR	aACR	aACR
$X_P Y(0)$	$\nearrow \infty$	$\nearrow \infty$	aACR	$\nearrow \infty$	ACR	$\nearrow \infty$	$\nearrow \infty$
$XTY_P(0)$	$\nearrow \infty$	$\nearrow \infty$	aACR	$\nearrow \infty$	ACR	$\nearrow \infty$	$\nearrow \infty$

Table S1: Summary of steady-state concentration responses for the network obtained by adding a reverse reaction for $X_P Y \rightarrow X + Y_P$ in the unmodified network (Figure 3a). The yellow-colored cells mean their steady-state behaviors are changed from the unmodified network, while transparent cells have the same steady-state behaviors as the unmodified network (see Table 1 in the main text). Notably, *all* the steady-state behaviors maintained after this modification.

	X^{SS}	XT^{SS}	X_P^{SS}	Y^{SS}	Y_P^{SS}	$X_P Y^{SS}$	XTY_P^{SS}
$X(0)$	aACR	aACR	$\nearrow \infty$	$\searrow 0$	aACR	aACR	aACR
$XT(0)$	aACR	aACR	$\nearrow \infty$	$\searrow 0$	aACR	aACR	aACR
$X_P(0)$	aACR	aACR	$\nearrow \infty$	$\searrow 0$	aACR	aACR	aACR
$Y(0)$	$\searrow 0$	$\searrow 0$	$\searrow 0$	$\nearrow \infty$	$\nearrow \infty$	$\searrow 0$	aACR
$Y_P(0)$	$\searrow 0$	$\searrow 0$	$\searrow 0$	$\nearrow \infty$	$\nearrow \infty$	$\searrow 0$	aACR
$X_P Y(0)$	$\nearrow \infty$	$\nearrow \infty$	aACR	$\nearrow \infty$	$\nearrow \infty$	$\nearrow \infty$	$\nearrow \infty$
$XTY_P(0)$	$\nearrow \infty$	$\nearrow \infty$	aACR	$\nearrow \infty$	$\nearrow \infty$	$\nearrow \infty$	$\nearrow \infty$

Table S2: Summary of steady-state concentration responses for the network obtained by adding a reverse reaction for $XTY_P \rightarrow XT + Y$ in the unmodified network (Figure 3a). The yellow-colored cells mean their steady-state behaviors are changed from the unmodified network, while transparent cells have the same steady-state behaviors as the unmodified network (see Table 1 in the main text).

	X^{ss}	XT^{ss}	X_P^{ss}	Y^{ss}	Y_P^{ss}	$X_P Y^{ss}$	XTY_P^{ss}
$X(0)$	$\nearrow \infty$	$\nearrow \infty$	$\nearrow \infty$	$\searrow 0$	$\searrow 0$	aACR	aACR
$XT(0)$	$\nearrow \infty$	$\nearrow \infty$	$\nearrow \infty$	$\searrow 0$	$\searrow 0$	aACR	aACR
$X_P(0)$	$\nearrow \infty$	$\nearrow \infty$	$\nearrow \infty$	$\searrow 0$	$\searrow 0$	aACR	aACR
$Y(0)$	$\searrow 0$	$\searrow 0$	$\searrow 0$	$\nearrow \infty$	$\nearrow \infty$	aACR	aACR
$Y_P(0)$	$\searrow 0$	$\searrow 0$	$\searrow 0$	$\nearrow \infty$	$\nearrow \infty$	aACR	aACR
$X_P Y(0)$	$\nearrow \infty$	$\nearrow \infty$	$\nearrow \infty$	$\nearrow \infty$	$\nearrow \infty$	$\nearrow \infty$	$\nearrow \infty$
$XTY_P(0)$	$\nearrow \infty$	$\nearrow \infty$	$\nearrow \infty$	$\nearrow \infty$	$\nearrow \infty$	$\nearrow \infty$	$\nearrow \infty$

Table S3: Summary of steady-state concentration responses for the network obtained by adding reverse reactions for all of the three irreversible reactions in the unmodified network (Figure 3a). The yellow-colored cells mean their steady-state behaviors are changed from the unmodified network, while transparent cells have the same steady-state behaviors as the unmodified network (see Table 1 in the main text).

	X^{ss}	XT^{ss}	XD^{ss}	X_P^{ss}	Y^{ss}	Y_P^{ss}	$X_P Y^{ss}$	XDY_P^{ss}
$X(0)$	aACR	aACR	aACR	$\nearrow \infty$	$\searrow 0$	ACR	aACR	aACR
$XT(0)$	aACR	aACR	aACR	$\nearrow \infty$	$\searrow 0$	ACR	aACR	aACR
$XD(0)$	aACR	aACR	aACR	$\nearrow \infty$	$\searrow 0$	ACR	aACR	aACR
$X_P(0)$	aACR	aACR	aACR	$\nearrow \infty$	$\searrow 0$	ACR	aACR	aACR
$Y(0)$	aACR	aACR	aACR	$\searrow 0$	$\nearrow \infty$	ACR	aACR	aACR
$Y_P(0)$	aACR	aACR	aACR	$\searrow 0$	$\nearrow \infty$	ACR	aACR	aACR
$X_P Y(0)$	$\nearrow \infty$	$\nearrow \infty$	$\nearrow \infty$	aACR	$\nearrow \infty$	ACR	$\nearrow \infty$	$\nearrow \infty$
$XTY_P(0)$	$\nearrow \infty$	$\nearrow \infty$	$\nearrow \infty$	aACR	$\nearrow \infty$	ACR	$\nearrow \infty$	$\nearrow \infty$

Table S4: Summary of steady-state concentration responses for the unmodified network in Figure S1a.

	X^{ss}	XT^{ss}	XD^{ss}	X_P^{ss}	Y^{ss}	Y_P^{ss}	$X_P Y^{ss}$	XDY_P^{ss}
$X(0)$	$\nearrow \infty$	$\nearrow \infty$	$\nearrow \infty$	$\nearrow \infty$	$\searrow 0$	$\searrow 0$	aACR	aACR
$XT(0)$	$\nearrow \infty$	$\nearrow \infty$	$\nearrow \infty$	$\nearrow \infty$	$\searrow 0$	$\searrow 0$	aACR	aACR
$XD(0)$	$\nearrow \infty$	$\nearrow \infty$	$\nearrow \infty$	$\nearrow \infty$	$\searrow 0$	$\searrow 0$	aACR	aACR
$X_P(0)$	$\nearrow \infty$	$\nearrow \infty$	$\nearrow \infty$	$\nearrow \infty$	$\searrow 0$	$\searrow 0$	aACR	aACR
$Y(0)$	aACR	aACR	aACR	$\searrow 0$	$\nearrow \infty$	aACR	aACR	aACR
$Y_P(0)$	aACR	aACR	aACR	$\searrow 0$	$\nearrow \infty$	aACR	aACR	aACR
$X_P Y(0)$	$\nearrow \infty$	$\nearrow \infty$	$\nearrow \infty$	aACR	$\nearrow \infty$	aACR	$\nearrow \infty$	$\nearrow \infty$
$XTY_P(0)$	$\nearrow \infty$	$\nearrow \infty$	$\nearrow \infty$	aACR	$\nearrow \infty$	aACR	$\nearrow \infty$	$\nearrow \infty$

Table S5: Summary of steady-state concentration responses for the network obtained by adding a reverse reaction for $XT \rightarrow X_P$ in the unmodified network (Figure S1a). The yellow-colored cells mean their steady-state behaviors are changed from the unmodified network, while transparent cells have the same steady-state behaviors as the unmodified network (see Table S4.)

	X^{SS}	XT^{SS}	XD^{SS}	X_P^{SS}	Y^{SS}	Y_P^{SS}	$X_P Y^{SS}$	$XD Y_P^{SS}$
$X(0)$	aACR	aACR	aACR	$\nearrow \infty$	$\searrow 0$	ACR	aACR	aACR
$XT(0)$	aACR	aACR	aACR	$\nearrow \infty$	$\searrow 0$	ACR	aACR	aACR
$XD(0)$	aACR	aACR	aACR	$\nearrow \infty$	$\searrow 0$	ACR	aACR	aACR
$X_P(0)$	aACR	aACR	aACR	$\nearrow \infty$	$\searrow 0$	ACR	aACR	aACR
$Y(0)$	aACR	aACR	aACR	$\searrow 0$	$\nearrow \infty$	ACR	aACR	aACR
$Y_P(0)$	aACR	aACR	aACR	$\searrow 0$	$\nearrow \infty$	ACR	aACR	aACR
$X_P Y(0)$	$\nearrow \infty$	$\nearrow \infty$	$\nearrow \infty$	aACR	$\nearrow \infty$	ACR	$\nearrow \infty$	$\nearrow \infty$
$XD Y_P(0)$	$\nearrow \infty$	$\nearrow \infty$	$\nearrow \infty$	aACR	$\nearrow \infty$	ACR	$\nearrow \infty$	$\nearrow \infty$

Table S6: Summary of steady-state concentration responses for the network obtained by adding a reverse reaction for $X_P Y \rightarrow X + Y_P$ in the unmodified network (Figure S1a). The yellow-colored cells mean their steady-state behaviors are changed from the unmodified network, while transparent cells have the same steady-state behaviors as the unmodified network (see Table S4.) Notably, *all* the steady-state behaviors maintained after this modification.

	X^{SS}	XT^{SS}	XD^{SS}	X_P^{SS}	Y^{SS}	Y_P^{SS}	$X_P Y^{SS}$	$XD Y_P^{SS}$
$X(0)$	aACR	aACR	aACR	$\nearrow \infty$	$\searrow 0$	aACR	aACR	aACR
$XT(0)$	aACR	aACR	aACR	$\nearrow \infty$	$\searrow 0$	aACR	aACR	aACR
$XD(0)$	aACR	aACR	aACR	$\nearrow \infty$	$\searrow 0$	aACR	aACR	aACR
$X_P(0)$	aACR	aACR	aACR	$\nearrow \infty$	$\searrow 0$	aACR	aACR	aACR
$Y(0)$	$\searrow 0$	$\searrow 0$	$\searrow 0$	$\searrow 0$	$\nearrow \infty$	$\nearrow \infty$	$\searrow 0$	aACR
$Y_P(0)$	$\searrow 0$	$\searrow 0$	$\searrow 0$	$\searrow 0$	$\nearrow \infty$	$\nearrow \infty$	$\searrow 0$	aACR
$X_P Y(0)$	$\nearrow \infty$	$\nearrow \infty$	$\nearrow \infty$	aACR	$\nearrow \infty$	$\nearrow \infty$	$\nearrow \infty$	$\nearrow \infty$
$XD Y_P(0)$	$\nearrow \infty$	$\nearrow \infty$	$\nearrow \infty$	aACR	$\nearrow \infty$	$\nearrow \infty$	$\nearrow \infty$	$\nearrow \infty$

Table S7: Summary of steady-state concentration responses for the network obtained by adding a reverse reaction for $XD Y_P \rightarrow XD + Y$ in the unmodified network (Figure S1a). The yellow-colored cells mean their steady-state behaviors are changed from the unmodified network, while transparent cells have the same steady-state behaviors as the unmodified network (see Table S4.)

	X^{SS}	XT^{SS}	XD^{SS}	X_P^{SS}	Y^{SS}	Y_P^{SS}	$X_P Y^{SS}$	$XD Y_P^{SS}$
$X(0)$	$\nearrow \infty$	$\nearrow \infty$	$\nearrow \infty$	$\nearrow \infty$	$\searrow 0$	$\searrow 0$	aACR	aACR
$XT(0)$	$\nearrow \infty$	$\nearrow \infty$	$\nearrow \infty$	$\nearrow \infty$	$\searrow 0$	$\searrow 0$	aACR	aACR
$XD(0)$	$\nearrow \infty$	$\nearrow \infty$	$\nearrow \infty$	$\nearrow \infty$	$\searrow 0$	$\searrow 0$	aACR	aACR
$X_P(0)$	$\nearrow \infty$	$\nearrow \infty$	$\nearrow \infty$	$\nearrow \infty$	$\searrow 0$	$\searrow 0$	aACR	aACR
$Y(0)$	$\searrow 0$	$\searrow 0$	$\searrow 0$	$\searrow 0$	$\nearrow \infty$	$\nearrow \infty$	aACR	aACR
$Y_P(0)$	$\searrow 0$	$\searrow 0$	$\searrow 0$	$\searrow 0$	$\nearrow \infty$	$\nearrow \infty$	aACR	aACR
$X_P Y(0)$	$\nearrow \infty$	$\nearrow \infty$	$\nearrow \infty$	$\nearrow \infty$	$\nearrow \infty$	$\nearrow \infty$	$\nearrow \infty$	$\nearrow \infty$
$XD Y_P(0)$	$\nearrow \infty$	$\nearrow \infty$	$\nearrow \infty$	$\nearrow \infty$	$\nearrow \infty$	$\nearrow \infty$	$\nearrow \infty$	$\nearrow \infty$

Table S8: Summary of steady-state concentration responses for the network obtained by adding reverse reactions for all of the three irreversible reactions in the unmodified network (Figure S1a). The yellow-colored cells mean their steady-state behaviors are changed from the unmodified network, while transparent cells have the same steady-state behaviors as the unmodified network (see Table S4.)

	E^{SS}	I^{SS}	I_P^{SS}	$E I_P^{SS}$	$E I_P I^{SS}$
$E(0)$	$\nearrow \infty$	ACR	$\searrow 0$	aACR	aACR
$I(0)$	$\searrow 0$	ACR	$\nearrow \infty$	aACR	aACR
$I_P(0)$	$\searrow 0$	ACR	$\nearrow \infty$	aACR	aACR
$E I_P(0)$	$\nearrow \infty$	ACR	aACR	$\nearrow \infty$	$\nearrow \infty$
$E I_P I(0)$	$\nearrow \infty$	ACR	aACR	$\nearrow \infty$	$\nearrow \infty$

Table S9: Summary of steady-state concentration responses for the unmodified network in Figure S1b.

	E^{ss}	I^{ss}	I_P^{ss}	EI_P^{ss}	$EI_P I^{ss}$
$E(0)$	$\nearrow \infty$	$\searrow 0$	$\searrow 0$	aACR	$\searrow 0$
$I(0)$	$\searrow 0$	aACR	$\nearrow \infty$	aACR	aACR
$I_P(0)$	$\searrow 0$	aACR	$\nearrow \infty$	aACR	aACR
$EI_P(0)$	$\nearrow \infty$	aACR	aACR	$\nearrow \infty$	$\nearrow \infty$
$EI_P I(0)$	$\nearrow \infty$	aACR	aACR	$\nearrow \infty$	$\nearrow \infty$

Table S10: Summary of steady-state concentration responses for the network obtained by adding a reverse reaction for $EI_P \rightarrow E + I$ in the unmodified network (Figure S1b). The yellow-colored cells mean their steady-state behaviors are changed from the unmodified network, while transparent cells have the same steady-state behaviors as the unmodified network (see Table S9.)

	E^{ss}	I^{ss}	I_P^{ss}	EI_P^{ss}	$EI_P I^{ss}$
$E(0)$	$\nearrow \infty$	aACR	$\searrow 0$	aACR	aACR
$I(0)$	$\searrow 0$	$\nearrow \infty$	$\nearrow \infty$	$\searrow 0$	aACR
$I_P(0)$	$\searrow 0$	$\nearrow \infty$	$\nearrow \infty$	$\searrow 0$	aACR
$EI_P(0)$	$\nearrow \infty$	aACR	aACR	$\nearrow \infty$	$\nearrow \infty$
$EI_P I(0)$	$\nearrow \infty$	aACR	aACR	$\nearrow \infty$	$\nearrow \infty$

Table S11: Summary of steady-state concentration responses for the network obtained by adding a reverse reaction for $EI_P I \rightarrow EI_P + I_P$ in the unmodified network (Figure S1b). The yellow-colored cells mean their steady-state behaviors are changed from the unmodified network, while transparent cells have the same steady-state behaviors as the unmodified network (see Table S9.)

	E^{ss}	I^{ss}	I_P^{ss}	EI_P^{ss}	$EI_P I^{ss}$
$E(0)$	$\nearrow \infty$	$\searrow 0$	$\searrow 0$	aACR	$\searrow 0$
$I(0)$	$\searrow 0$	$\nearrow \infty$	$\nearrow \infty$	$\searrow 0$	aACR
$I_P(0)$	$\searrow 0$	$\nearrow \infty$	$\nearrow \infty$	$\searrow 0$	aACR
$EI_P(0)$	$\nearrow \infty$	aACR	aACR	$\nearrow \infty$	$\nearrow \infty$
$EI_P I(0)$	$\nearrow \infty$	aACR	aACR	$\nearrow \infty$	$\nearrow \infty$

Table S12: Summary of steady-state concentration responses for the network obtained by adding reverse reactions for all of the two irreversible reactions in the unmodified network (Figure S1b). The yellow-colored cells mean their steady-state behaviors are changed from the unmodified network, while transparent cells have the same steady-state behaviors as the unmodified network (see Table S9.)

	S^{ss}	P^{ss}	E^{ss}	F^{ss}	SE^{ss}	PF^{ss}
$S(0)$	$\nearrow \infty$	$\nearrow \infty$	$\searrow 0$	$\searrow 0$	aACR	aACR
$P(0)$	$\nearrow \infty$	$\nearrow \infty$	$\searrow 0$	$\searrow 0$	aACR	aACR
$E(0)$	$\searrow 0$	aACR	$\nearrow \infty$	aACR	aACR	aACR
$F(0)$	aACR	$\searrow 0$	aACR	$\nearrow \infty$	aACR	aACR
$SE(0)$	$\searrow 0$	$\nearrow \infty$	$\nearrow \infty$	$\searrow 0$	aACR	aACR
$PF(0)$	$\nearrow \infty$	$\searrow 0$	$\searrow 0$	$\nearrow \infty$	aACR	aACR

Table S13: Summary of steady-state concentration responses for the unmodified network in Figure S1c. The left-top 2×4 block changes depending on the parameter values. Other possibilities are the following: (aACR, $\nearrow \infty$, aACR, $\searrow 0$) and ($\nearrow \infty$, aACR, $\searrow 0$, aACR).

	S^{SS}	P^{SS}	E^{SS}	F^{SS}	SE^{SS}	PF^{SS}
$S(0)$	$\nearrow \infty$	$\nearrow \infty$	$\searrow 0$	$\searrow 0$	aACR	aACR
$P(0)$	$\nearrow \infty$	$\nearrow \infty$	$\searrow 0$	$\searrow 0$	aACR	aACR
$E(0)$	$\searrow 0$	$\searrow 0$	$\nearrow \infty$	aACR	aACR	$\searrow 0$
$F(0)$	aACR	$\searrow 0$	aACR	$\nearrow \infty$	aACR	aACR
$SE(0)$	$\nearrow \infty$	$\nearrow \infty$	$\nearrow \infty$	$\searrow 0$	$\nearrow \infty$	aACR
$PF(0)$	$\nearrow \infty$	$\searrow 0$	$\searrow 0$	$\nearrow \infty$	aACR	aACR

Table S14: Summary of steady-state concentration responses the network obtained by adding a reverse reaction for $SE \rightarrow P + E$ in the unmodified network (Figure S1c). The yellow-colored cells mean their steady-state behaviors are changed from the unmodified network, while transparent cells have the same steady-state behaviors as the unmodified network (see Table S13.)

	S^{SS}	P^{SS}	E^{SS}	F^{SS}	SE^{SS}	PF^{SS}
$S(0)$	$\nearrow \infty$	$\nearrow \infty$	$\searrow 0$	$\searrow 0$	aACR	aACR
$P(0)$	$\nearrow \infty$	$\nearrow \infty$	$\searrow 0$	$\searrow 0$	aACR	aACR
$E(0)$	$\searrow 0$	aACR	$\nearrow \infty$	aACR	aACR	aACR
$F(0)$	$\searrow 0$	$\searrow 0$	aACR	$\nearrow \infty$	$\searrow 0$	aACR
$SE(0)$	$\searrow 0$	$\nearrow \infty$	$\nearrow \infty$	$\searrow 0$	aACR	aACR
$PF(0)$	$\nearrow \infty$	$\nearrow \infty$	$\searrow 0$	$\nearrow \infty$	aACR	$\nearrow \infty$

Table S15: Summary of steady-state concentration responses the network obtained by adding a reverse reaction for $PF \rightarrow S + F$ in the unmodified network (Figure S1c). The yellow-colored cells mean their steady-state behaviors are changed from the unmodified network, while transparent cells have the same steady-state behaviors as the unmodified network (see Table S13.)

	S^{SS}	P^{SS}	E^{SS}	F^{SS}	SE^{SS}	PF^{SS}
$S(0)$	$\nearrow \infty$	$\nearrow \infty$	$\searrow 0$	$\searrow 0$	aACR	aACR
$P(0)$	$\nearrow \infty$	$\nearrow \infty$	$\searrow 0$	$\searrow 0$	aACR	aACR
$E(0)$	$\searrow 0$	$\searrow 0$	$\nearrow \infty$	aACR	aACR	$\searrow 0$
$F(0)$	$\searrow 0$	$\searrow 0$	aACR	$\nearrow \infty$	$\searrow 0$	aACR
$SE(0)$	$\nearrow \infty$	$\nearrow \infty$	$\nearrow \infty$	$\searrow 0$	$\nearrow \infty$	aACR
$PF(0)$	$\nearrow \infty$	$\nearrow \infty$	$\searrow 0$	$\nearrow \infty$	aACR	$\nearrow \infty$

Table S16: Summary of steady-state concentration responses the network obtained by adding reverse reactions for all of the two irreversible reactions in the unmodified network (Figure S1c). The yellow-colored cells mean their steady-state behaviors are changed from the unmodified network, while transparent cells have the same steady-state behaviors as the unmodified network (see Table S13.)

	W^{SS}	W^{*SS}	Z^{SS}	Z^{*SS}	E_1^{SS}	E_2^{SS}	E_3^{SS}	WE_1^{SS}	$W^*E_2^{SS}$	ZW^{*SS}	$Z^*E_3^{SS}$
$W(0)$	aACR	$\nearrow \infty$	$\searrow 0$	aACR	aACR	$\searrow 0$	aACR	aACR	aACR	aACR	aACR
$W^*(0)$	aACR	$\nearrow \infty$	$\searrow 0$	aACR	aACR	$\searrow 0$	aACR	aACR	aACR	aACR	aACR
$Z(0)$	aACR	aACR	aACR	$\nearrow \infty$	aACR	aACR	$\searrow 0$	aACR	aACR	aACR	aACR
$Z^*(0)$	aACR	aACR	aACR	$\nearrow \infty$	aACR	aACR	$\searrow 0$	aACR	aACR	aACR	aACR
$E_1(0)$	$\searrow 0$	aACR	aACR	aACR	$\nearrow \infty$	aACR	aACR	aACR	aACR	aACR	aACR
$E_2(0)$	$\searrow 0$	aACR	aACR	aACR	$\nearrow \infty$	aACR	aACR	aACR	aACR	aACR	aACR
$E_3(0)$	aACR	aACR	aACR	$\searrow 0$	aACR	aACR	$\nearrow \infty$	aACR	aACR	aACR	aACR
$WE_1(0)$	$\searrow 0$	$\nearrow \infty$	$\searrow 0$	aACR	$\nearrow \infty$	$\searrow 0$	aACR	aACR	aACR	aACR	aACR
$W^*E_2(0)$	$\nearrow \infty$	$\searrow 0$	$\searrow 0$	aACR	$\nearrow \infty$	$\searrow 0$	aACR	aACR	aACR	aACR	aACR
$ZW^*(0)$	aACR	$\nearrow \infty$	$\searrow 0$	$\nearrow \infty$	aACR	$\searrow 0$	$\searrow 0$	aACR	aACR	aACR	aACR
$Z^*E_3(0)$	$\searrow 0$	$\searrow 0$	$\nearrow \infty$	$\searrow 0$	aACR	aACR	$\nearrow \infty$	$\searrow 0$	$\searrow 0$	aACR	aACR

Table S17: Summary of steady-state concentration responses for the unmodified network in Figure S1d. Many of the entries depend on parameter values, and a complete characterization of all possible steady-state responses has not been done due to the large number of varying parameters. Nevertheless, it is evident that the majority of species exhibit aACR behavior. See Table S18 for an alternative set of results.

	W^{SS}	W^{*SS}	Z^{SS}	Z^{*SS}	E_1^{SS}	E_2^{SS}	E_3^{SS}	WE_1^{SS}	$W^*E_2^{SS}$	ZW^{*SS}	$Z^*E_3^{SS}$
$W(0)$	$\nearrow \infty$	aACR	aACR	aACR	$\searrow 0$	aACR	aACR	aACR	aACR	aACR	aACR
$W^*(0)$	$\nearrow \infty$	aACR	aACR	aACR	$\searrow 0$	aACR	aACR	aACR	aACR	aACR	aACR
$Z(0)$	aACR	aACR	aACR	$\nearrow \infty$	aACR	aACR	$\searrow 0$	aACR	aACR	aACR	aACR
$Z^*(0)$	aACR	aACR	aACR	$\nearrow \infty$	aACR	aACR	$\searrow 0$	aACR	aACR	aACR	aACR
$E_1(0)$	$\searrow 0$	aACR	aACR	aACR	$\nearrow \infty$	aACR	$\searrow 0$	aACR	aACR	aACR	aACR
$E_2(0)$	aACR	$\searrow 0$	aACR	$\searrow 0$	aACR	$\nearrow \infty$	aACR	aACR	aACR	$\searrow 0$	$\searrow 0$
$E_3(0)$	aACR	aACR	aACR	$\searrow 0$	aACR	aACR	$\nearrow \infty$	aACR	aACR	aACR	aACR
$WE_1(0)$	$\searrow 0$	$\nearrow \infty$	$\searrow 0$	aACR	$\nearrow \infty$	$\searrow 0$	aACR	aACR	aACR	aACR	aACR
$W^*E_2(0)$	$\nearrow \infty$	$\searrow 0$	aACR	$\searrow 0$	$\searrow 0$	$\nearrow \infty$	aACR	aACR	aACR	$\searrow 0$	$\searrow 0$
$ZW^*(0)$	$\nearrow \infty$	$\nearrow \infty$	$\searrow 0$	$\nearrow \infty$	$\searrow 0$	$\searrow 0$	$\searrow 0$	aACR	aACR	aACR	aACR
$Z^*E_3(0)$	$\searrow 0$	$\searrow 0$	$\nearrow \infty$	$\searrow 0$	aACR	aACR	$\nearrow \infty$	$\searrow 0$	$\searrow 0$	aACR	aACR

Table S18: Summary of steady-state concentration responses for the unmodified network in Figure S1d. Many of the entries depend on parameter values. Nevertheless, it is evident that the majority of species exhibit aACR behavior. See Table S17 for an alternative set of results.

References

- [1] J. Bochnak, M. Coste, and M.-F. Roy, *Real algebraic geometry*, vol. 36. Springer Science & Business Media, 2013.
- [2] M. Coste, *An introduction to semialgebraic geometry*. Istituti editoriali e poligrafici internazionali, 2000.
- [3] G. Shinar and M. Feinberg, “Structural sources of robustness in biochemical reaction networks,” *Science*, vol. 327, no. 5971, pp. 1389–1391, 2010.
- [4] C. Conradi and C. Pantea, “Multistationarity in biochemical networks: results, analysis, and examples,” in *Algebraic and combinatorial computational biology*, pp. 279–317, Elsevier, 2019.
- [5] A. Goldbeter and D. E. Koshland Jr, “An amplified sensitivity arising from covalent modification in biological systems,” *Proceedings of the National Academy of Sciences*, vol. 78, no. 11, pp. 6840–6844, 1981.
- [6] B. N. Kholodenko, “Negative feedback and ultrasensitivity can bring about oscillations in the mitogen-activated protein kinase cascades,” *European journal of biochemistry*, vol. 267, no. 6, pp. 1583–1588, 2000.